ROYAL INSTITUTE
OF TECHNOLOGY

Accurate evaluation of layer potentials in integral equations

Anna-Karin Tornberg
KTH Mathematics, Stockholm

SIAM Annual Meeting, July 10-14, 2017.

FLOW
LINNÉ FLOW CENTRE

SeRC

Integral equations in microfluidics

- Increased interest in microfluidic applications, both due to manufactured microfluidic devices and applications in biology.
- At this small scales, Stokes equations are applicable.
- Linear elliptic PDEs such as Stokes equations can be reformulated as boundary integral equations.
- In droplet based micro fluidics: drops stabilized by surfactant not to coalesce.

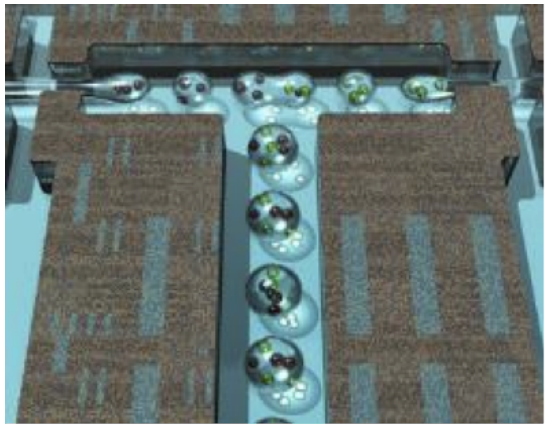

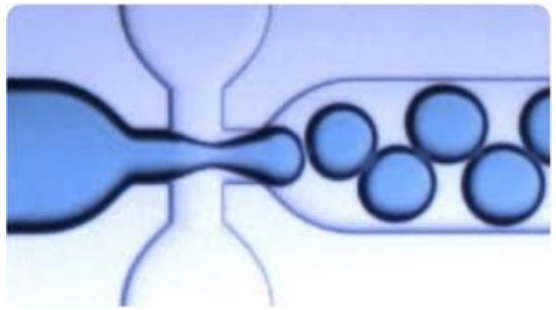

Droplet based microfluidics – a powerful technology with future potential

Pictures courtesy of the lab of Helene Andersson-Svahn, KTH.

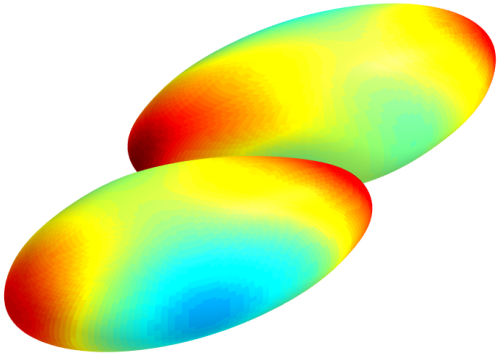

Stokes equations

$$\mu \Delta \boldsymbol{u} = \nabla p, \qquad \nabla \cdot \boldsymbol{u} = 0$$

$\boldsymbol{u}$ velocity, p pressure.

For drop with surface $\partial\Omega_m$:

Jump condition at interface $\partial\Omega_m$ for normal stress:

$$\tau\hat{n}|^{exterior} - \tau\hat{n}|^{interior} = \sigma\kappa\hat{\boldsymbol{n}}$$

τ : stress tensor σ : surface tension coefficient

κ : mean curvature $\hat{\boldsymbol{n}}$: outward unit normal vector

Outer fluid viscosity μ_0/ drop viscosity μ_d enters $\tau\hat{n}|^{exterior}/\tau\hat{n}|^{interior}$

Formula above for clean drop.
With surfactants, the interfacial force $\boldsymbol{f} = \sigma\kappa\hat{\boldsymbol{n}}$ will be modified.

Green's functions/Fundamental solutions

- The major fundamental solution or free space Green's function for the Stokes equations is the so-called Stokeslet.

3D: $$S_{ij}(\boldsymbol{x}-\boldsymbol{y}) = \frac{\delta_{ij}}{|\boldsymbol{x}-\boldsymbol{y}|} + \frac{(x_i - y_i)(x_j - y_j)}{|\boldsymbol{x}-\boldsymbol{y}|^3}, \qquad i,j = 1,2,3.$$

2D: $$S_{ij}(\boldsymbol{x}-\boldsymbol{y}) = -\delta_{ij}\log|\boldsymbol{x}-\boldsymbol{y}| + \frac{(x_i - y_i)(x_j - y_j)}{|\boldsymbol{x}-\boldsymbol{y}|^2}, \qquad i,j = 1,2.$$

- There is also the Stresslet.

3D: $$T_{ijk}(\boldsymbol{x}-\boldsymbol{y}) = -6\frac{(x_i - y_i)(x_j - y_j)(x_k - y_k)}{|\boldsymbol{x}-\boldsymbol{y}|^5}, \qquad i,j,k = 1,2,3.$$

2D: $$T_{ijk}(\boldsymbol{x}-\boldsymbol{y}) = -4\frac{(x_i - y_i)(x_j - y_j)(x_k - y_k)}{|\boldsymbol{x}-\boldsymbol{y}|^4}, \qquad i,j,k = 1,2.$$

Immiscible two-phase flow (drops)

Interface condition: $\tau\hat{n}|^{exterior} - \tau\hat{n}|^{interior} = \sigma\kappa\hat{\boldsymbol{n}}$

τ : stress tensor $\quad$ σ : surface tension coefficient

κ : curvature $\quad$ $\hat{\boldsymbol{n}}$: outward unit normal vector

$\lambda = \mu/\mu_0$

Ratio of viscosity (drops/outer fluid)

For any point $\boldsymbol{x}$ on a drop boundary $\Gamma_m, m = 1, \cdots, M$

$$\boldsymbol{u}(\boldsymbol{x}) - 2\frac{\lambda-1}{\lambda+1}\boldsymbol{K}[\boldsymbol{u}](\boldsymbol{x}) = \frac{2}{\lambda+1}(-\boldsymbol{S}\,[\sigma\kappa\hat{\boldsymbol{n}}](\boldsymbol{x}) + \boldsymbol{u}_\infty(\boldsymbol{x}))$$

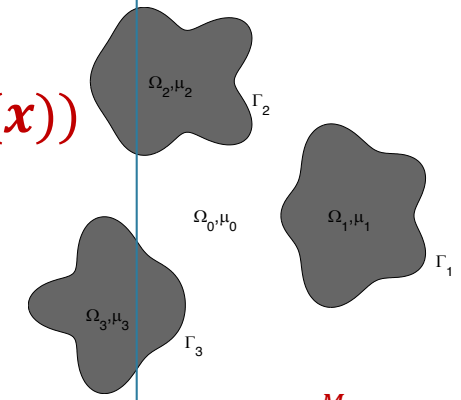

where

$$\boldsymbol{S}[\boldsymbol{f}](\boldsymbol{x}) = \frac{1}{8\pi\mu_0}\sum_{m=1}^{M}\int_{\Gamma_m}\boldsymbol{f}(\boldsymbol{y})\cdot S(\boldsymbol{x}-\boldsymbol{y})\,\boldsymbol{dS_y}$$

$$\Gamma = \bigcup_{m=1}^{M}\Gamma_m$$

$$\boldsymbol{K}_D[\boldsymbol{u}](\boldsymbol{x}) = \frac{1}{8\pi\mu_0}\sum_{m=1}^{M}\int_{\Gamma_m}\boldsymbol{u}(\boldsymbol{y})\cdot T(\boldsymbol{x}-\boldsymbol{y})\cdot\hat{\boldsymbol{n}}(\boldsymbol{y})\,\boldsymbol{dS_y}$$

S: Stokeslet

T : Stresslet

Boundary integral equations and discretizations

- Discretization by a Nyström method
  - Collocation points = quadrature points
  - Accuracy of the numerical scheme = accuracy of the quadrature method
- Reducing the number of unknowns – discretizing only the boundaries of the domain, not the volume.

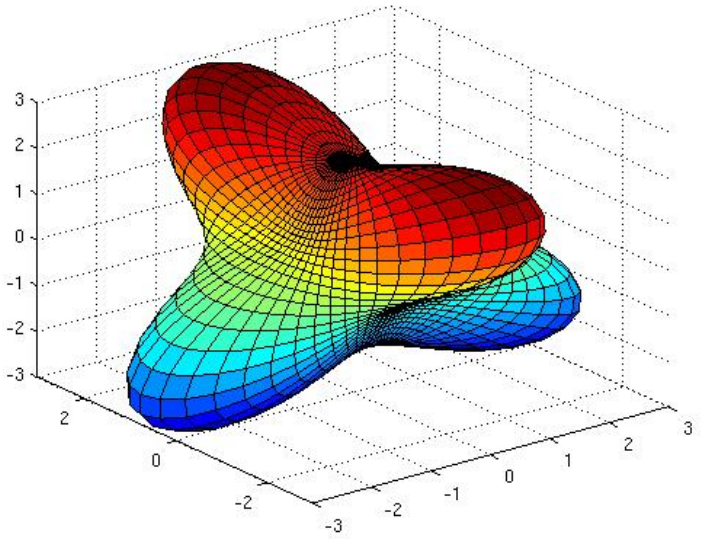

- Second kind integral equation: condition number of system matrix does not increase with refinement.

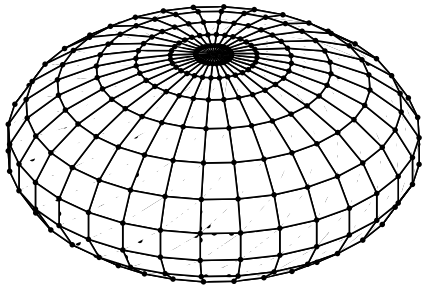

This implies:

- Number of iterations with e.g. GMRES constant with refinement.
- Computational complexity scales as cost of matrix vector multiply.

Main challenge for Integral Methods (1/2): Dense matrices

- Slow decay of fundamental solutions yield *full (dense) system matrices.* $O(N^2)$ cost for matrix-vector multiply.

The 3D Stokeslet ($\hat{\boldsymbol{r}} = \boldsymbol{r}/|\boldsymbol{r}|$)

$$S(\boldsymbol{r}) = \frac{1}{|\boldsymbol{r}|}(1 + \hat{\boldsymbol{r}}\hat{\boldsymbol{r}})$$

- *Fast summation methods* needed.
  - Fast multipole methods (FMM) and FFT based methods.
  - Combined with iterative methods, such as GMRES, total work reduced to O(N log N) for well conditioned integral formulations.

- Our contribution: The Spectral Ewald Methods.
  A set of *spectrally accurate FFT based fast methods*.
  - Based on so called Ewald summation.
  - Triply periodic most natural, for Stokeslet, Stresslet, Rotlet.
  - Extended also to domains with periodicity in one and two of the three directions, and recently also for non-periodic domains.
  - Work with D. Lindbo, L. af Klinteberg and D. S. Shamshirgar.

Main challenges for Integral Methods (2/2): Quadrature

The 3D Stokeslet : $S(\boldsymbol{r}) = \frac{1}{|r|}(1 + \hat{\boldsymbol{r}}\hat{\boldsymbol{r}}),\ \hat{\boldsymbol{r}} = \boldsymbol{r}/|\boldsymbol{r}|.$

$\int_{\partial\Omega} S(\boldsymbol{x} - \boldsymbol{y})\, \boldsymbol{f}(\boldsymbol{y})\, \mathrm{d}\boldsymbol{S}_y$

- Integral singular at $\boldsymbol{x} = \boldsymbol{y}$.
- $\boldsymbol{x}$ close to surface: Nearly singular.

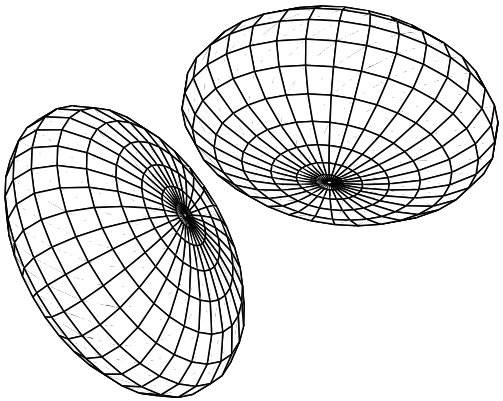

Integral nearly singular at close interactions

- We will have integrals containing both the Stokeslet and the Stresslet.
- Special quadrature methods needed!
- Currently a very active research field.

- Our contributions:
  - Highly accurate method based on Gauss-Legendre quadrature for 2D drops (w R. Ojala).
  - Development of Quadrature by Expansion (QBX) w L. af Klinteberg, M. Siegel.
  - Will discuss this today.

The interior Laplace problem

- Interior Laplace problem in 2D, with Dirichlet BCs.

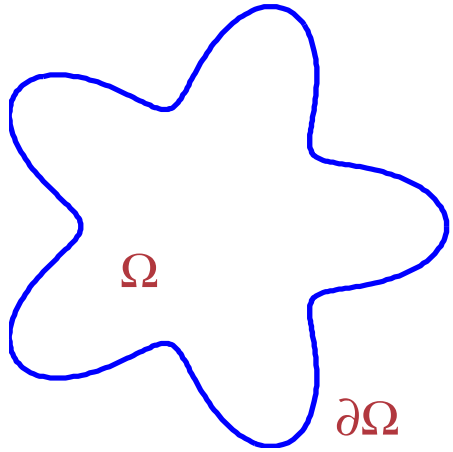

The solution for any point $x \in \Omega$ can be represented with

$$\varphi(\boldsymbol{x}) = D[\mu](\boldsymbol{x}) = \frac{1}{2\pi} \int_{\partial\Omega} \mu(\boldsymbol{y}) \frac{\partial}{\partial n_y} \log(|\boldsymbol{x} - \boldsymbol{y}|) \mathrm{d}S(\boldsymbol{y})$$

The double layer density μ is the solution of the integral equation:

$$\frac{1}{2}\mu(\boldsymbol{x}) + \frac{1}{2\pi} \int_{\partial\Omega} \mu(\boldsymbol{y}) \frac{\partial}{\partial n_y} \log(|\boldsymbol{x} - \boldsymbol{y}|) \mathrm{d}S(\boldsymbol{y}) = g(\boldsymbol{x}), \qquad \boldsymbol{x} \in \partial\Omega$$

where g is the Dirichlet data.

$\Gamma = \partial\Omega$,
assumed smooth.

This is obtained by using the limit

$$\lim_{\substack{z \to x \in \partial\Omega \\ z \in \Omega}} D[\mu](\boldsymbol{x}) = \frac{1}{2}\mu(\boldsymbol{x}) + D[\mu](\boldsymbol{x})$$

This integral equation can also be formulated in complex variables, and we will use that formulation in the following.

The interior Laplace problem (complex variable formulation)

The double layer density μ is the solution of the integral equation:

$$\frac{1}{2}\mu(z) + \frac{1}{2\pi}\int_{\partial\Omega} \mu(\tau)\mathrm{Im}\left\{\frac{\mathrm{d}\,\tau}{\tau - z}\right\} = g(z), \qquad z \in \mathbb{C}, z \in \partial\Omega$$

where g is the Dirichlet data.

- Finite limit as $\tau \to z$ exists.
- Discretized with a Nyström method.
- 16-point Gauss-Legendre panels.
- Solved with high accuracy to find the double layer density μ on the boundary (w GMRES and FMM).
- Well conditioned matrix, discretization of second kind integral equation.

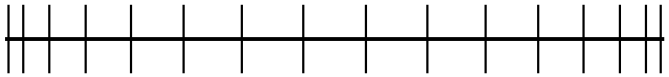

Distribution of points,
16-point Gauss-Legendre rule.

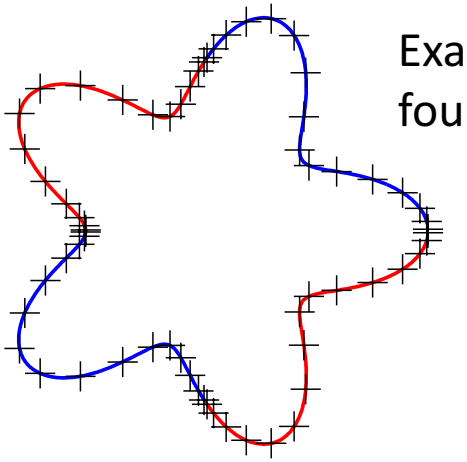

Example with four panels.

Error in solution of the Laplace equation

The solution at any point $z \in \Omega$ can be evaluated as:

$$\varphi(z) = D[\mu](z) = \frac{1}{2\pi} \int_{\partial\Omega} \mu(\tau) \mathrm{Im}\left\{\frac{\mathrm{d}\,\tau}{\tau - z}\right\}$$

Discretized with 16 point Gauss-Legendre panels.

Colors: Measured numerical errors.

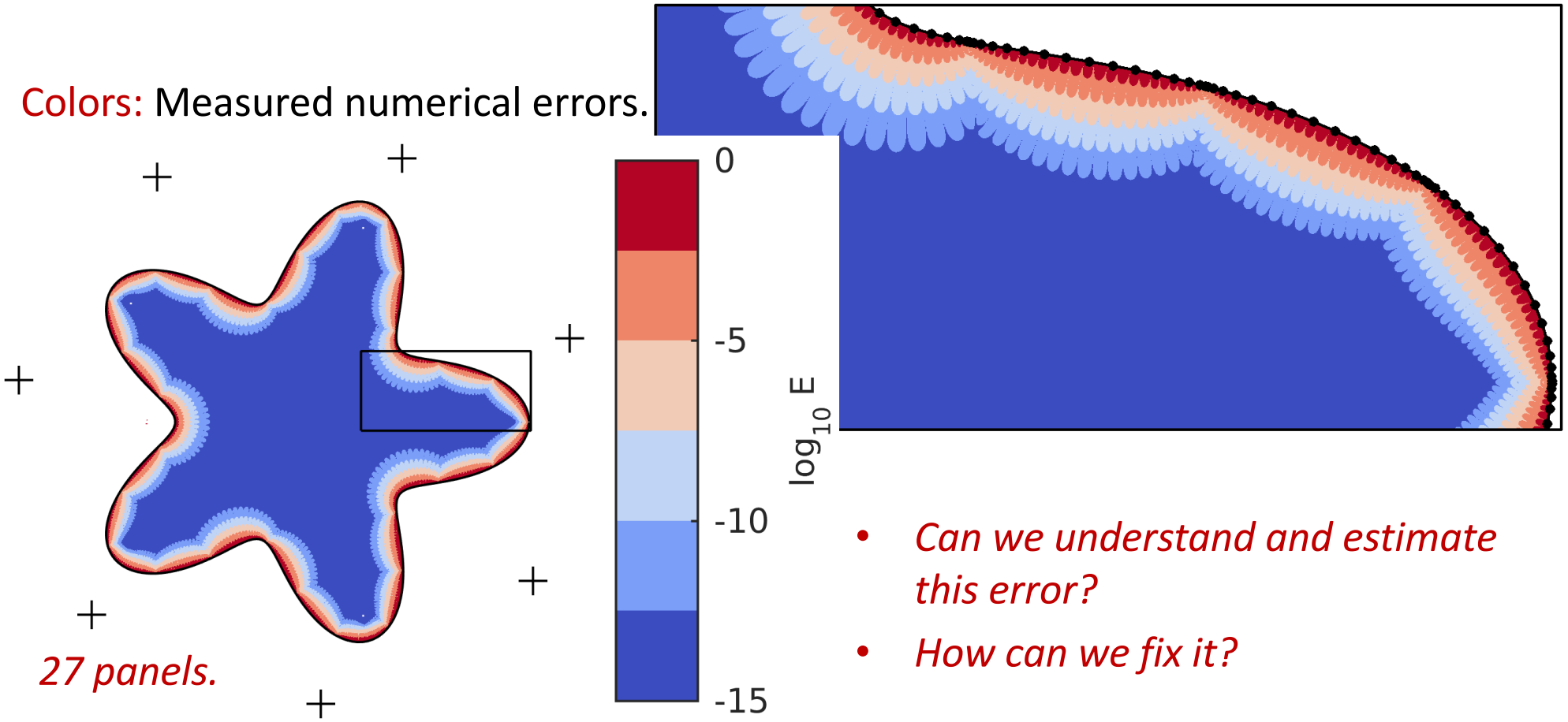

27 panels.

- *Can we understand and estimate this error?*
- *How can we fix it?*

A 1D example

$$\int_{-1}^{1} f(t)\,\mathrm{d}t, \qquad f(t) = \frac{1}{t^2 + \delta^2}$$

$$R_{16}[f] = \int_{-1}^{1} f(t)\,\mathrm{d}t - \sum_{i=1}^{16} w_i f(t_i),$$

16 point Gauss-Legendre quadrature rule

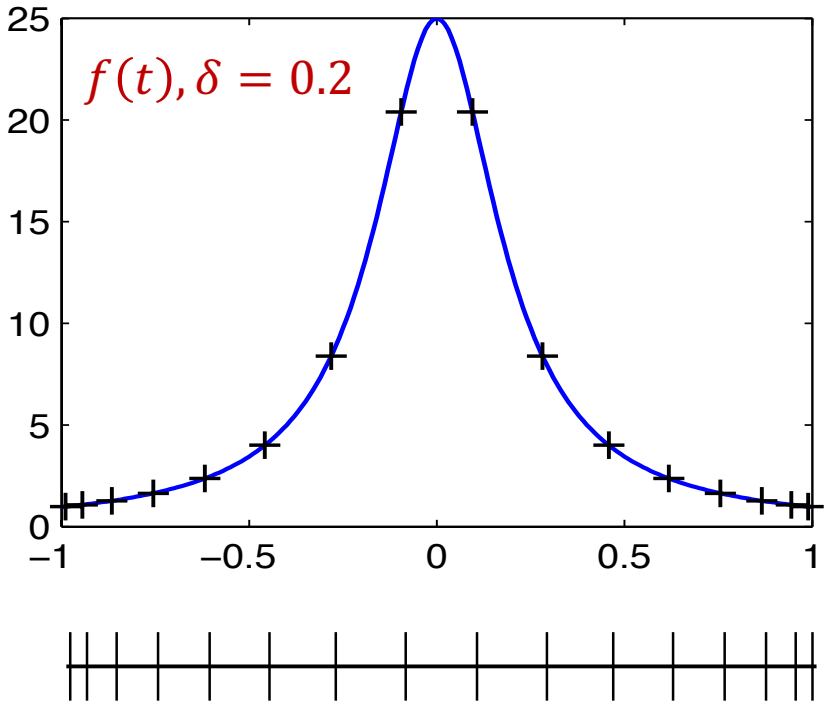

Error $|R_{16}[f]|$ vs δ^2

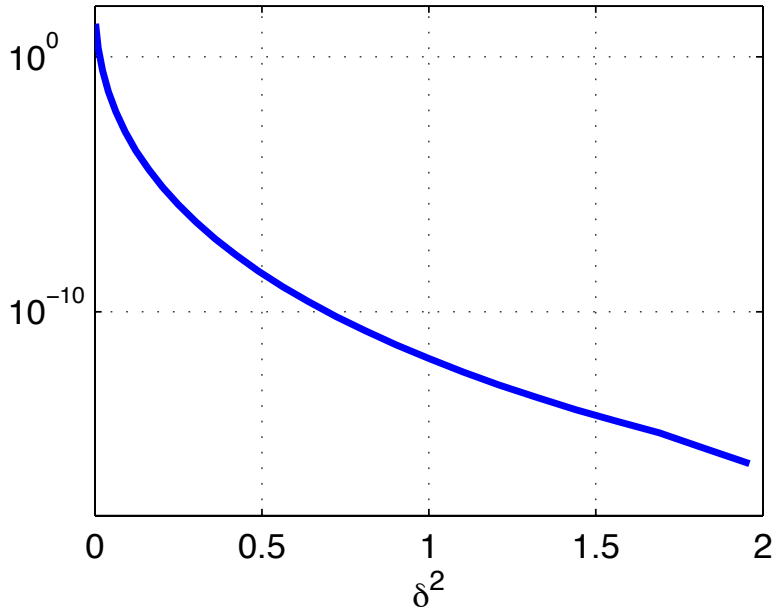

Classical error estimate

$$|R_n[f]| \leq \frac{L^{2n+1}(n!)^4}{(2n+1)[(2n)!]^3} \left\| f^{(2n)} \right\|_\infty$$

n - point Gauss-Legendre rule on interval of length L.
(integrates polynomials up to degree $2n-1$ exactly.

With $\left\| f^{(2n)} \right\|_\infty = \frac{(2n)!}{\delta^{2n+2}}$, and Stirlings formula for factorials

$$|R_n[f]| \leq \frac{4\pi}{\delta^2(2\delta)^{2n}} \left\| f^{(2n)} \right\|_\infty$$

Over estimates the error - especially for small δ
For $\delta < 0.5$

- error estimate grows exponentially with n.
- actual error decreases exponentially with n.

New error estimate

- Want error estimates for evaluating ($a, b \in \mathbb{R}, b > 0$, $p = 1,2, \ldots$)

$$\int_{-1}^{1} g_p(t)\,\mathrm{d}t = \int_{-1}^{1} \frac{1}{\left((t-a)^2 + b^2\right)^p}\,\mathrm{d}t.$$

$$\int_{-1}^{1} f_p(t)\,\mathrm{d}t = \int_{-1}^{1} \frac{1}{(t-t_0)^p}\,\mathrm{d}t, \qquad t_0 = a + ib,$$

- Assume an n-point Gauss-Legendre rule is used.

- Can use contour integrals and residue calculus (e.g. Donaldson end Elliott, 1972), to derive such an estimate.

- Aiming for practical estimates, not bounds!

Theorem for quadrature error

The error in the approximation of $\int_{-1}^{1} f_p(t)\,\mathrm{d}t$

$$f_p(t) = (t - t_0)^{-p}, \qquad t_0 = a + ib, \qquad a, b \in \mathbb{R}, b > 0$$

with the n-point Gauss-Legendre rule, is in the asymptotic limit $n \to \infty$

$$|R_n[f_p]| = \frac{2\pi}{(p-1)!} \left| \frac{2n+1}{\sqrt{t_0^2 - 1}} \right|^{p-1} \frac{1}{\left| t_0 + \sqrt{t_0^2 - 1} \right|^{2n+1}}$$

For $b \ll 1$ we have

$$|R_n[f_p]| < \sim \frac{2\pi}{(p-1)!} (2n)^{p-1} e^{-2bn}$$ as $n \to \infty$

Note exponential decay with n, also for small b.

af Klinteberg & T., Adv. Comput. Math, 2017.

Estimate for our 1D example

- Theorem with similar result for $g_p(t)$.
- Our earlier 1D-example: $f(t) = g_1(t)$, with $a = 0, b = \delta$.

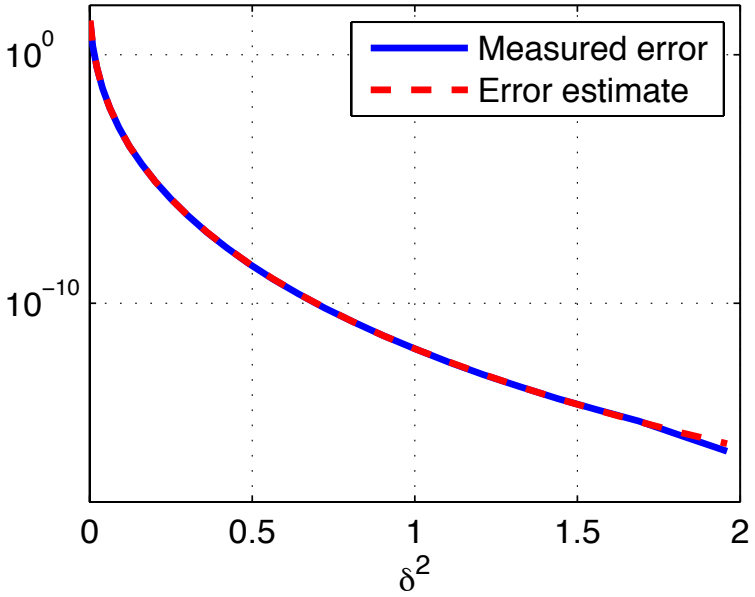

$$\int_{-1}^{1} g_1(t)dt, \qquad g_1(t) = \frac{1}{t^2 + \delta^2}$$

Error estimate for $n = 16$ $(z = \delta i)$

$$|R_{16}[g_1]| \cong \frac{1}{\delta}\left|\mathrm{Im}\left\{\frac{2\pi}{\left(z + \sqrt{z^2 - 1}\right)^{33}}\right\}\right|$$

- Estimate very accurate also for this moderate *n*.

Error in the complex plane

- Study the quadrature error for

$$\int_{-1}^{1} f_1(t)\,\mathrm{d}t = \int_{-1}^{1} \frac{\mathrm{d}t}{t - t_0},$$

  as a function of $t_0 \in \mathbb{C}$.
- Can view this as one flat panel between -1 and 1.

Error for $t_0 \in \mathbb{C}$.

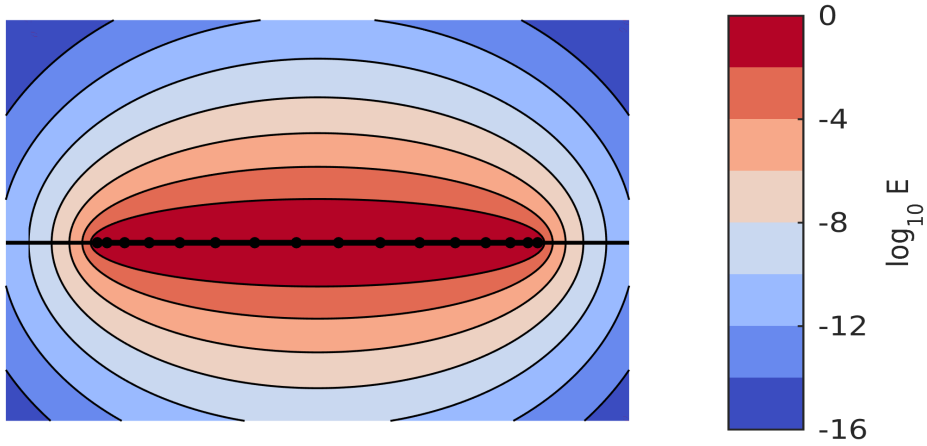

Colors: Measured numerical errors.

Black contours: Error estimate $e_{\text{est}}(t_0)$.

$$|R_{16}[f_1]| \cong e_{\text{est}}(t_0) = \frac{2\pi}{\left|t_0 + \sqrt{t_0^2 - 1}\right|^{33}}$$

The ellipses have foci in ± 1, and are known as Bernstein ellipses.

- 16 point Gauss-Legendre quadrature rule ($n = 16$).

Back to the Laplace equation

- Want to estimate the quadrature error for

$$\varphi(z_0) = \frac{1}{2\pi} \int_{\partial\Omega} \mu(\tau) \mathrm{Im}\left\{\frac{\mathrm{d}\,\tau}{\tau - z_0}\right\}, \qquad z_0 \in \Omega$$

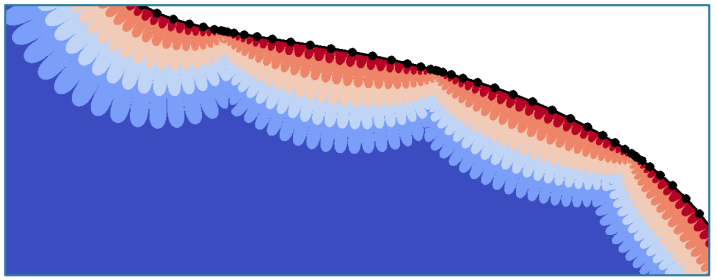

evaluated by a panel-based 16 point Gauss-Legendre quadrature rule.

- Denote by $e_i(z)$ the error from panel Γ_i.
- Total error:

$$e(z) = \sum_{i=1}^{N_{panels}} e_i(z)$$

In practice:
Enough to include contribution from two closest panels.

- Can use estimate for a flat panel to estimate the error for each panel.
  - Map the actual panel to a panel with end points at -1 and 1.
  - Map z_0 to t_0 using that mapping.
- Must include density μ in the estimate.

Estimate of Laplace solution error

- Simple mapping as if each panel is flat to determine t_0 from z_0.

$$e_{\text{est}}(t_0) = \frac{\|\mu\|_{L^\infty(\Gamma_i)}}{\left|t_0 + \sqrt{t_0^2 - 1}\right|^{2n+1}} \qquad n = 16$$

- Rather good estimate, but less so for panels far with higher curvature.

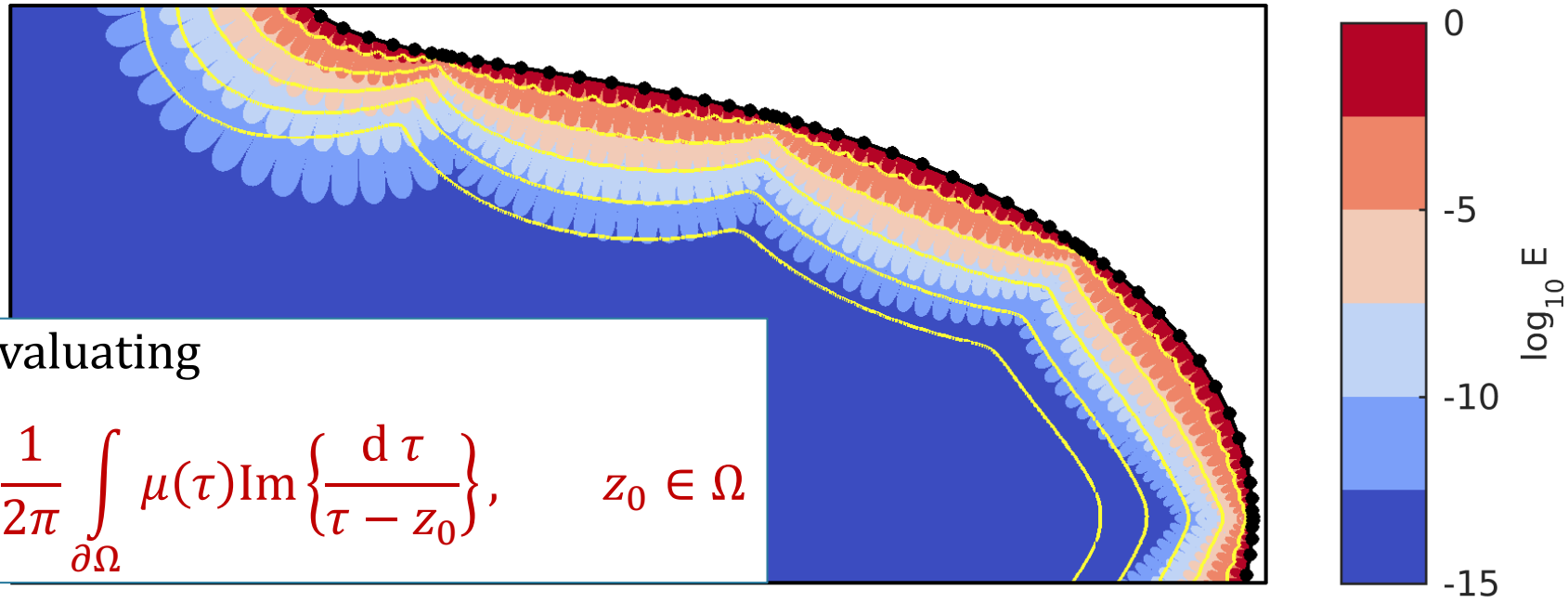

Error in evaluating

$$\varphi(z_0) = \frac{1}{2\pi} \int_{\partial\Omega} \mu(\tau) \operatorname{Im}\left\{\frac{\mathrm{d}\,\tau}{\tau - z_0}\right\}, \qquad z_0 \in \Omega$$

Colors: Measured numerical errors. Yellow contours: Error estimate.

A more accurate mapping

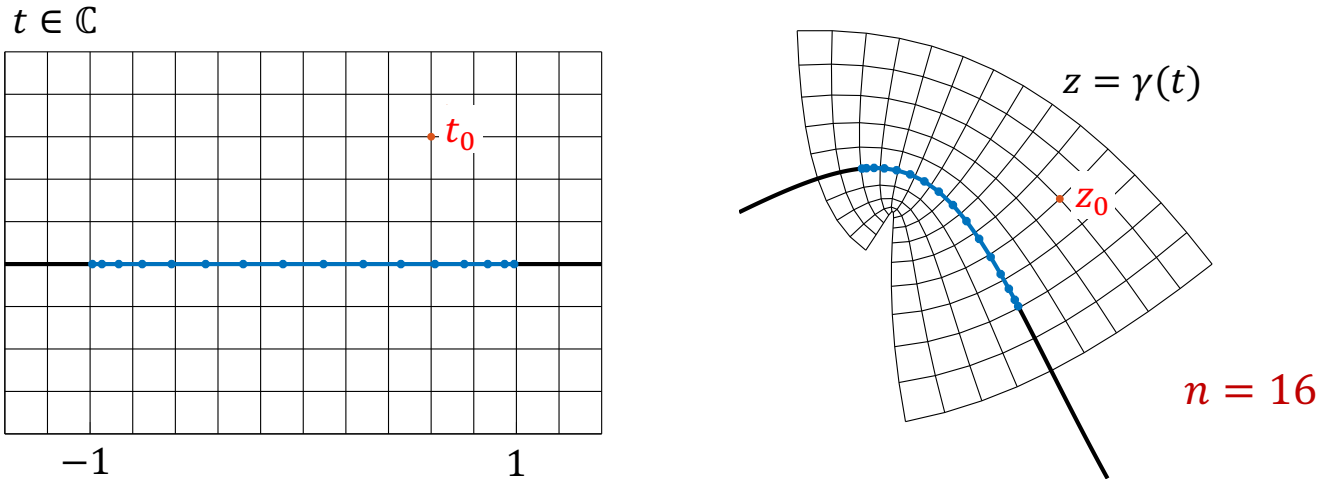

- Given target z_0 and nodes $\{z_i\}, i = 1, \ldots, n$ on panel, want to find t_0 such that ($\gamma(t)$ parameterization of panel),

$$z_0 = \gamma(t_0).$$

- Analytic continuation of γ approximated by Legendre interpolant:

$$\gamma(t) \approx P_n[\gamma](t) = \sum_{\ell=0}^{n-1} \hat{\gamma}_\ell P_\ell(t) \qquad \left(\hat{\gamma}_\ell = \frac{2\ell+1}{2} \sum_{i=1}^{n} P_\ell(t_i) w_i z_i \right)$$

- Solve for t_0 using Newton's method.

Error from one panel

- Study the quadrature error for

$$\int_\gamma \frac{1}{z - z_0}\,\mathrm{d}z$$

  as a function of z_0.
- Numerically solve for corresponding t_0.
- Use estimate for flat panel.

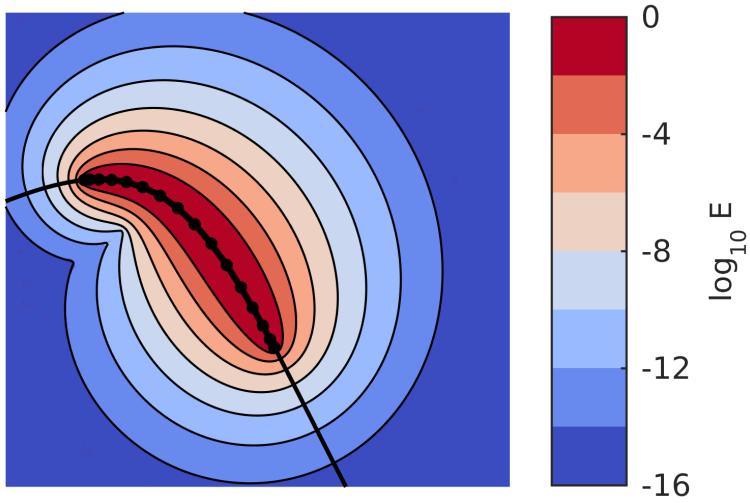

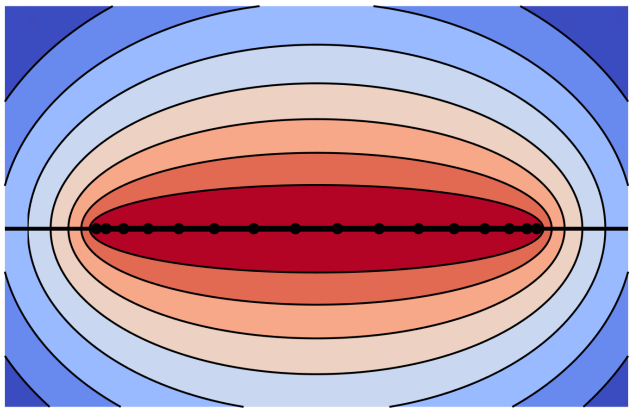

Colors: Measured numerical errors.

Black contours: Error estimate $e_{\mathrm{est}}(t_0)$.

$$|R_{16}[f_1]| \cong e_{\mathrm{est}}(t_0) = \frac{2\pi}{\left|t_0 + \sqrt{t_0^2 - 1}\right|^{33}}$$

Estimate of Laplace solution error

- For panel close to z_0, determine t_0 by Newton solve.
- To include density μ, form Legendre interpolant also for μ.
- Use estimate $e_{\text{est}}(t_0) = \left| \text{Im} \left[\frac{P_n[\mu](t_0)}{\left(t_0 + \sqrt{t_0^2 - 1} \right)^{2n+1}} \right] \right| \quad n = 16$

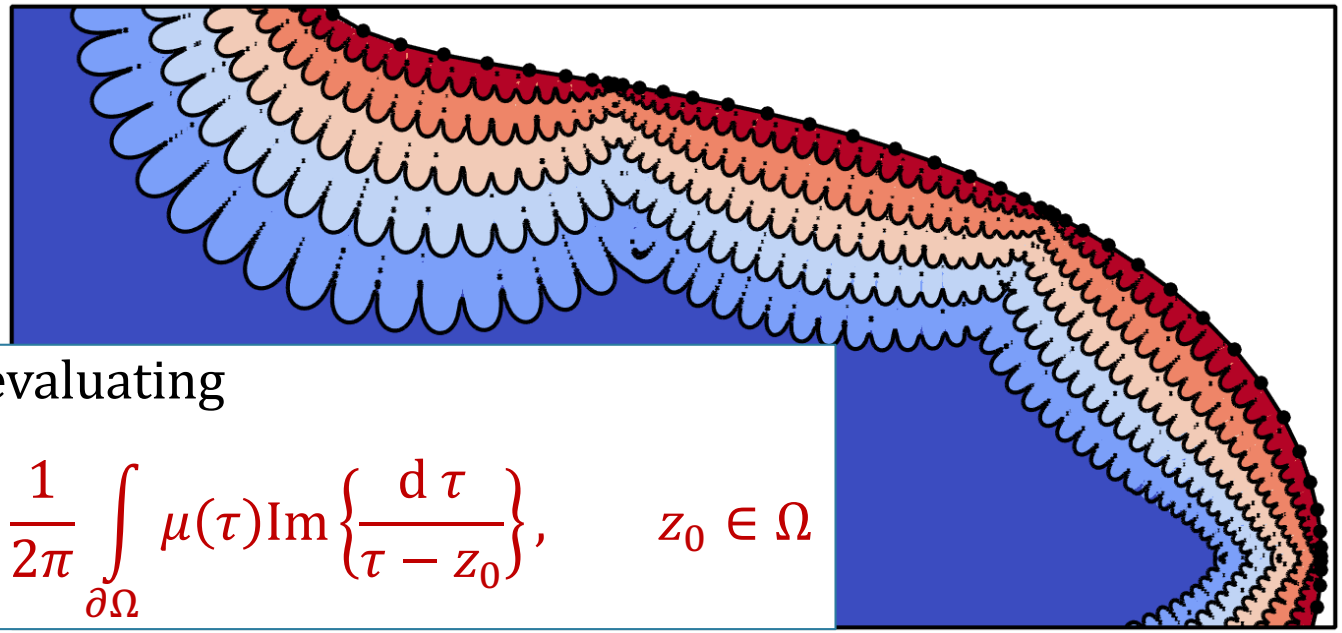

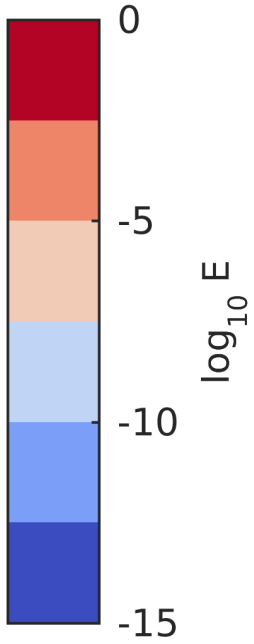

Error in evaluating

$$\varphi(z_0) = \frac{1}{2\pi} \int_{\partial\Omega} \mu(\tau) \text{Im} \left\{ \frac{\mathrm{d}\,\tau}{\tau - z_0} \right\}, \qquad z_0 \in \Omega$$

Colors: Measured numerical errors. Black contours: Error estimate.

The Helmholtz equation

- The Helmholtz equation $\Delta u + k^2 u = 0$

  has the fundamental solution $G_k(z_0, z) = \frac{i}{4} H_0^1(k|z_0 - z|)$

- Singularity at $z_0 = z$ is of log-type, can show that estimate for Laplace double layer holds also for Helmholtz double layer.

$$e_{\text{est}}(t_0) = \frac{\|\mu\|_{L^\infty(\Gamma_i)}}{\left|t_0 + \sqrt{t_0^2 - 1}\right|^{2n+1}}$$

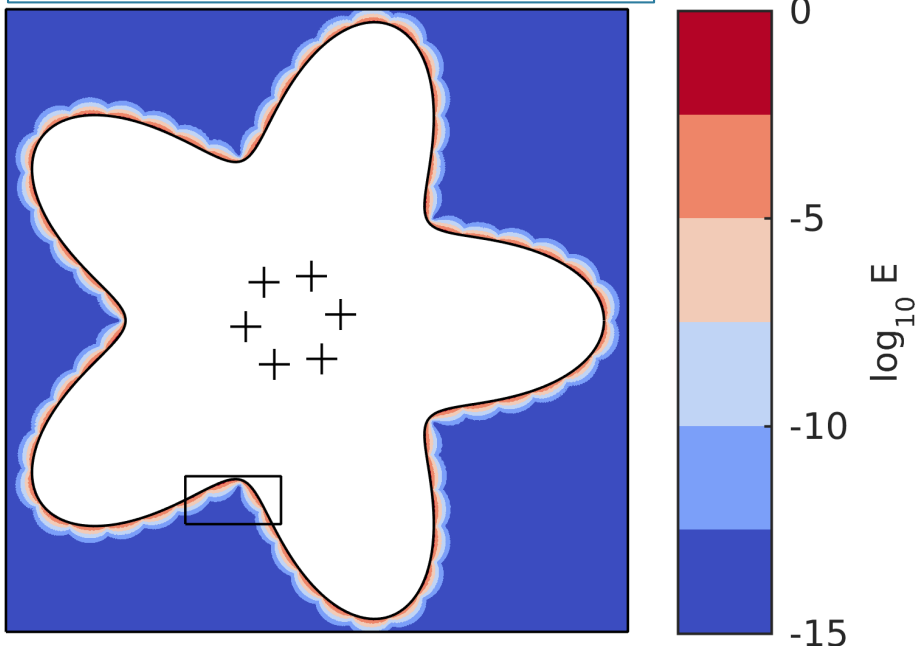

2D Helmholtz,

- exterior Dirichlet problem,
- Sommerfeld radiation condition.

Colors: Measured numerical errors.

Black contours: Error estimate.

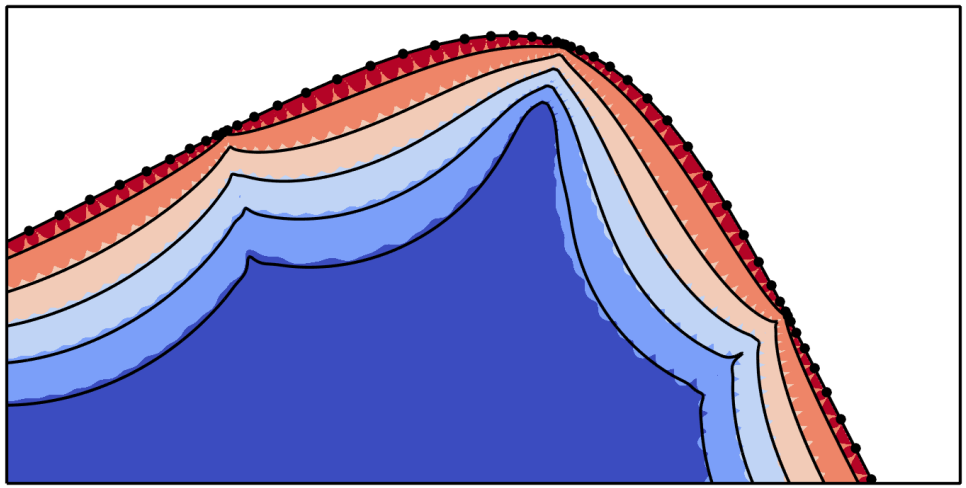

Quadrature approaches in 1D/2D

- Many people have worked with designing quadrature approaches for singular integrals, with techniques such as
  - Singularity subtraction (treat some piece analytically, reduce the singularity of what remains to be handled numerically).
  - Modified quadrature weights (specific kernel and geometry)
  - Change of variables that removes the principal singularity.
- Not as much has been done for nearly singular integrals, which is often more difficult.
- An excellent method for 2D was introduced by Helsing and Ojala (2008), handles both singular and near singular integrals efficiently to extremely high accuracy.

Some names: B. Alpert, T. Beale, G. Biros, J. Bremer, O. Bruno, M.G. Duffy, Z. Gimbutas, S. Kapur, R. Kress, J.N. Lyness, V. Rokhlin, A. Sidi, J. Strain, L. Ying, D. Zorin, and more….

Special interpolatory quadrature – ”Helsing – quadrature”

$$I(z) = \int_{\Gamma_j} \frac{f(\tau)\mathrm{d}\tau}{\tau - z} \approx \sum_{k=0}^{15} c_k \int_{-1}^{1} \frac{\tau^k \mathrm{d}\tau}{\tau - z_0} = \sum_{k=0}^{15} c_k p_k$$

- The $p_k : s$ can be evaluated analytically. Done by recursion once p_0 computed.
- Error in solution of the $c_k : s$ can be kept close to round-off.

- Complex scaling and translation to get end points of panel at -1 and 1.
- Second integral is over transformed panel Γ_j , z_0 is the transformed z.
- Solution of a Vandermonde system to find the expansion coefficients.
- Solve instead transposed system, with right hand side independent on values of f, depending only on z_0.
- This way, conditioning can be kept under control.

Technique can be applied to any kernel that can be integrated analytically when multiplied with a complex monomial.

Helsing and Ojala (2008)

Error in solution: Special quadrature method

$$\varphi(z) = \frac{1}{2\pi} \int_{\partial\Omega} \mu(\tau) \mathrm{Im}\left\{\frac{\mathrm{d}\,\tau}{\tau - z}\right\}$$

- Special quadrature used when evaluation point z "too close" to $\partial\Omega$.
- Interpolatory quadrature, Helsing and Ojala (2008).

Regular quadrature.

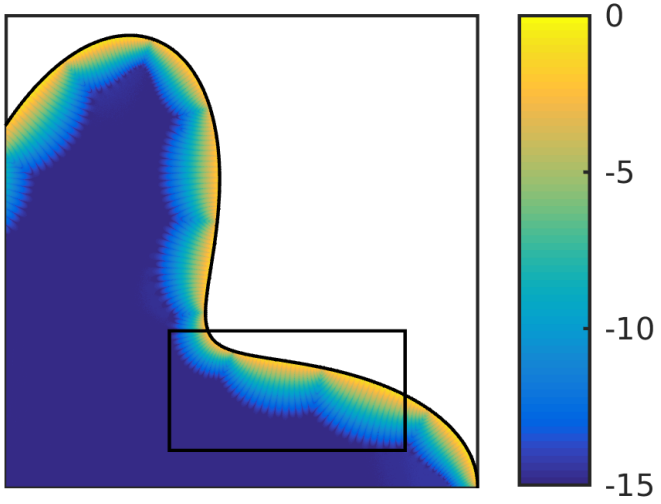

With special interpolatory quadrature.

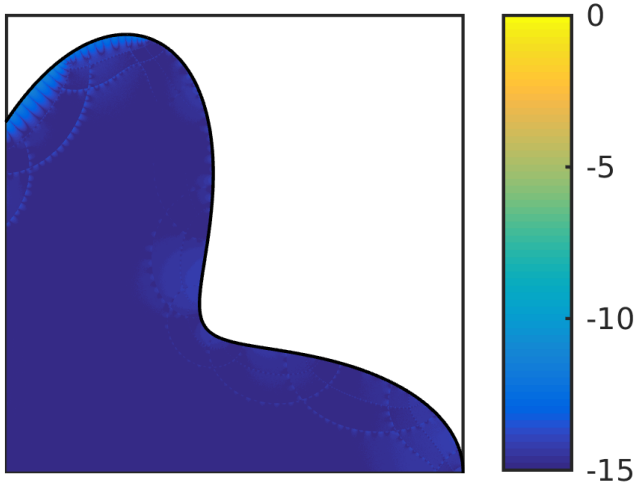

If μ on each panel approximated to round off with a 15^{th} degree polynomial in the complex variable, quadrature will be accurate to round off.

Stokes flow with drops in 2D

- Write integrals in complex form, apply interpolatory quadrature as needed.
- Extension of Helsing & Ojala, see Ojala & T. , JCP 2015.
- Many other components for full method, with time-stepping, arclength preserving tangential velocity, global spatial adaptivity….

Clean drops as black contours.

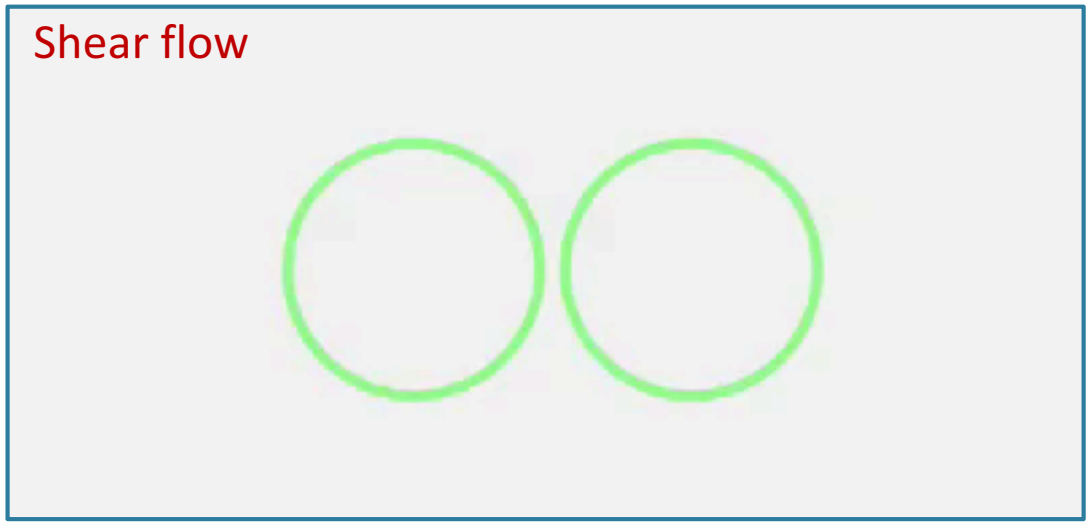

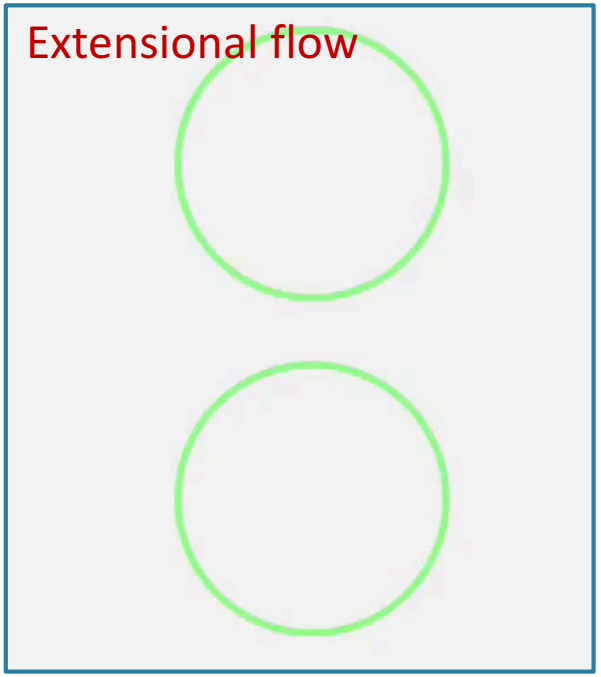

Colored contours show concentration of surfactant that has been added to modified the surface tension (not discussed here, with Sara Pålsson).

Quadrature by expansion (QBX)

- The interpolatory quadrature used in 2D does not naturally extend to 3D.
- Quadrature by Expansion (QBX) introduced by Klöckner et al (JCP, 2013) for the Helmholtz equation in 2D.
- A general idea that extends to 3D.

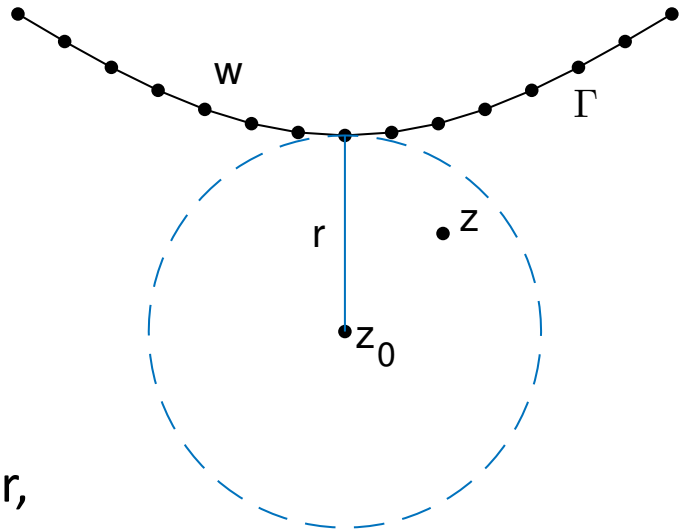

The idea is as follows:

- Even though the integral is nearly singular, the field that is produces is smooth.
- Create a local expansion around a center z_0 away from the boundary.
- The coefficients in the expansion will be evaluated using upsampled quadrature (will get to what that means).
- Evaluate the local expansion to obtain the result.

Start discussion in 2D for Laplace equation, before we move to Stokes in 3D.

Quadrature by expansion (QBX)

- The Green's function is split,

$$G(z,w) = \sum_{m=0}^{\infty} A_m(w,z_0)B_m(z,z_0)$$

for center z_0 such that $|z - z_0| < |w - z_0|$.

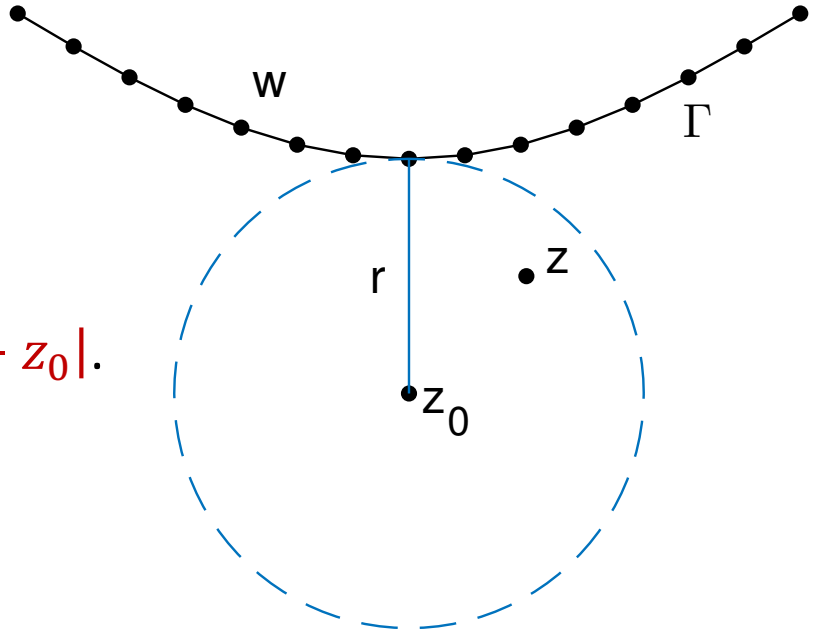

- For Laplace double layer in 2D

$$\varphi(z) = \frac{1}{2\pi}\int_{\Gamma} \mu(w)\,\mathrm{Im}\left\{\frac{\mathrm{d}\,w}{w-z}\right\}$$

we get

$$\varphi(z) = \mathrm{Im}\sum_{m=0}^{\infty} a_m(z-z_0)^m, \qquad a_m = \frac{1}{2\pi}\int_{\Gamma} \frac{\mu(w)}{(w-z_0)^{m+1}}\,\mathrm{d}\,w$$

- Coefficients a_m computed using upsampled quadrature,
  $\Longrightarrow$ approximation $\tilde{a}_m$

QBX error

- The error when truncating to p terms, and evaluating coefficients by quadrature:

$$\varphi(z) - \varphi_p(z) = \mathrm{Im} \sum_{m=0}^{\infty} a_m (z - z_0)^m - \mathrm{Im} \sum_{m=0}^{p} \tilde{a}_m (z - z_0)^m$$

$$= \underbrace{\mathrm{Im} \sum_{m=p+1}^{\infty} a_m (z - z_0)^m}_{\text{Truncation error } e_T} + \underbrace{\mathrm{Im} \sum_{m=0}^{p} (a_m - \tilde{a}_m)(z - z_0)^m}_{\text{Coefficient error } e_Q}$$

Typical error plot:

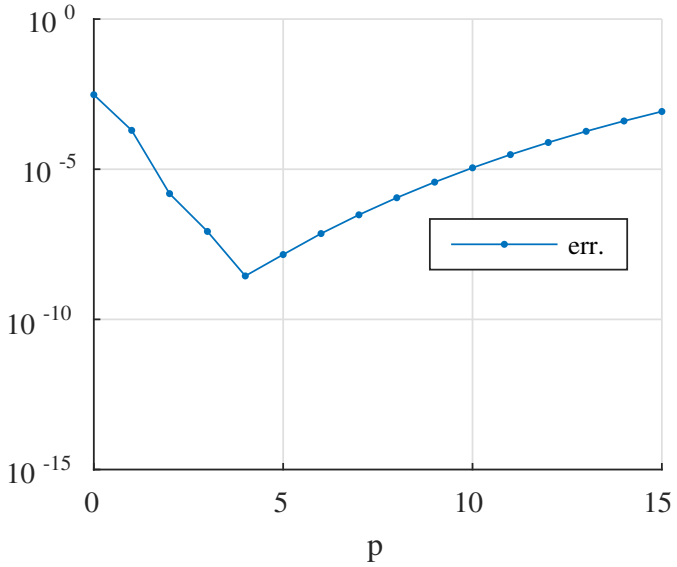

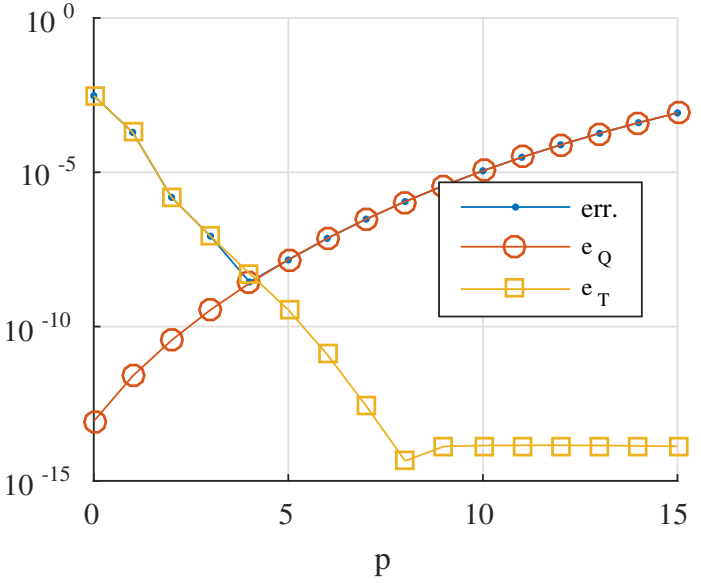

QBX error

- Truncation error e_T controlled by number of terms p.
- Coefficient error e_Q comes from numerically evaluating

$$a_m = \frac{1}{2\pi} \int_\Gamma \frac{\mu(w)}{(w - z_0)^{m+1}} \, \mathrm{d}\, w, \qquad m = 0, \ldots, p.$$

- Assuming μ well resolved on 16-point discretization of panel.
- Coefficients more difficult to evaluate as m increases.
- Evaluate using a higher order GL rule.
- Must interpolate μ to this finer GL grid on panel (upsample).

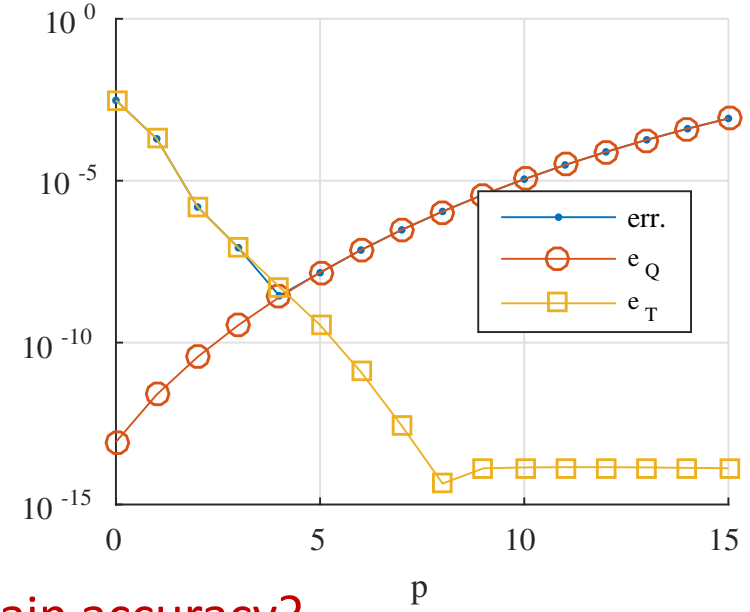

How high order GL rule is needed for a certain accuracy?
- Use error estimates.

Error from one panel - higher powers

- Study the quadrature error for $\int_\gamma \frac{1}{(z-z_0)^p}\,\mathrm{d}z$ as a function of z_0.
- From theorem for integral $\int_{-1}^{1} \frac{1}{(t-t_0)^p}\,\mathrm{d}t$ we have:

$$\left|R_n[f_p]\right| \cong e_{est}^{p}(t_0) = \frac{2\pi}{(p-1)!}\left|\frac{2n+1}{\sqrt{t_0^2-1}}\right|^{p-1} \frac{1}{\left|t_0+\sqrt{t_0^2-1}\right|^{2n+1}}$$

- Including also parameterization of a curved panel γ yields

$$e_{est}^{\gamma,p}(z_0) = \frac{e_{est}^{p}(t_0)}{\left(\gamma'(t_0)\right)^{p-1}}$$

(and hence $\gamma'(t_0)$ does not enter for $p = 1$).

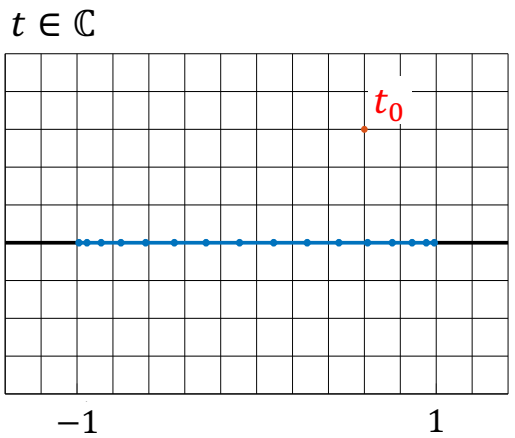

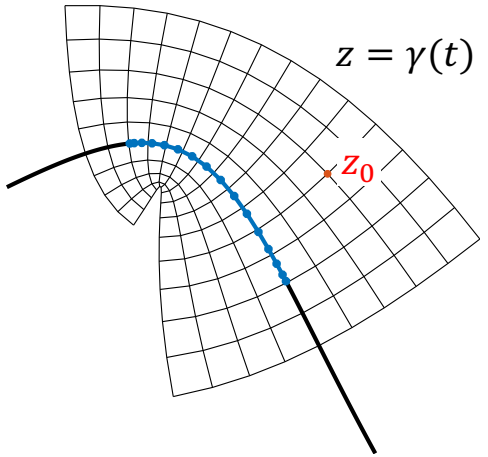

$z_0 = \gamma(t_0)$.

Error from one panel – higher powers

$$\int_\gamma \frac{1}{(z-z_0)^5}\,\mathrm{d}z$$

$n = 16$

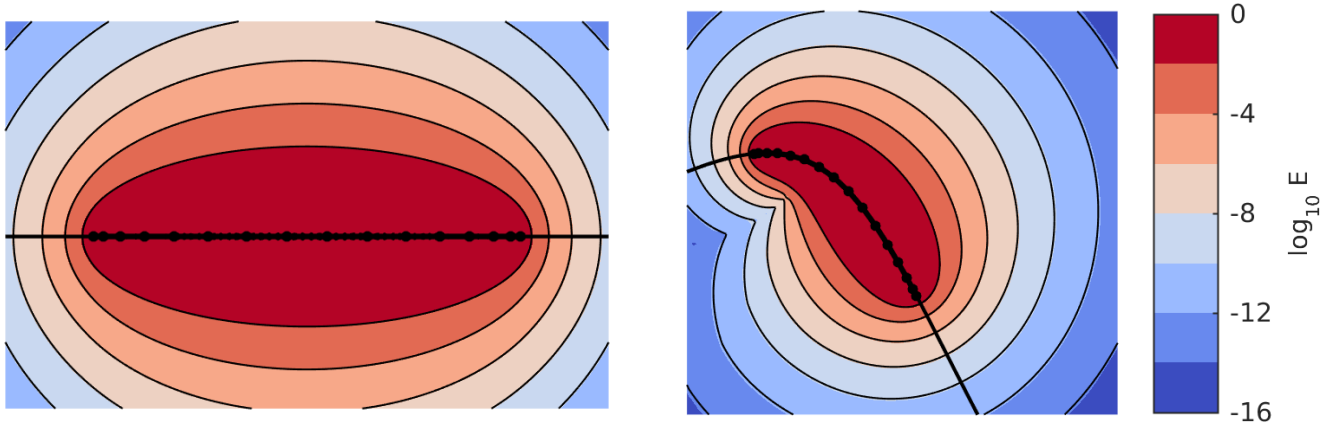

$$\int_\gamma \frac{1}{(z-z_0)^{10}}\,\mathrm{d}z$$

$n = 32$

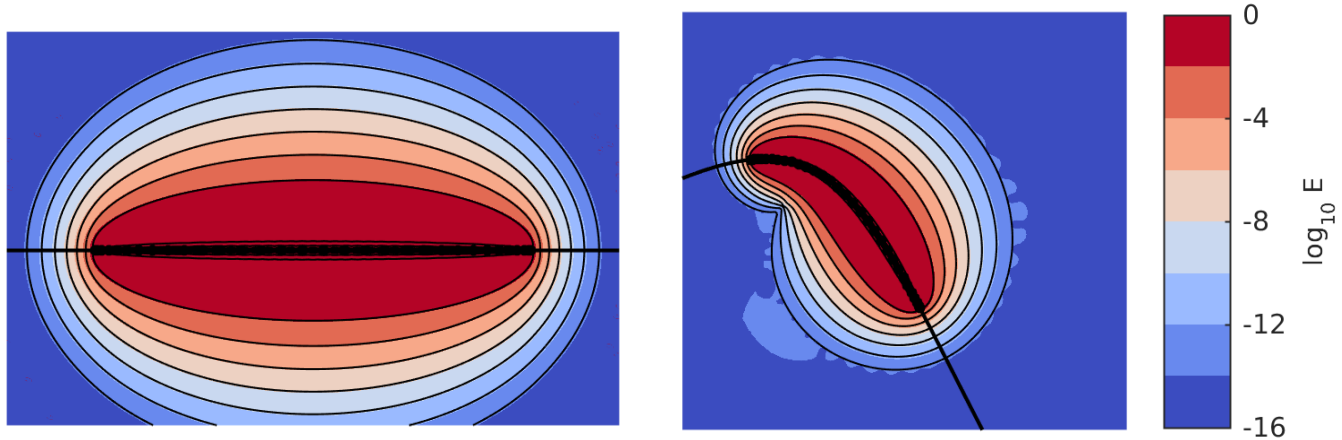

Colors: Measured numerical errors.

Black contours: Error estimate $e^{p}_{\mathrm{est}}(t_0)$ / $e^{\gamma,p}_{est}(z_0)$.

Local QBX expansions

- The double layer density $\mu(w)$ has been computed at the GL nodes at each panel ($n = 16$ nodes) and is assumed to be well resolved.

For a set of points $z \in \Omega$, we want to approximate

$$\varphi(z) = \frac{1}{2\pi} \int_{\Gamma} \mu(w) \mathrm{Im} \left\{ \frac{\mathrm{d}\, w}{w - z} \right\}$$

with an error no larger than a given tolerance *TOL*.

- Error estimate can for each z determine if regular quadrature will be sufficient for all panels.
- If not: form a ”local” QBX expansion including contributions from panels nearby the evaluation point.
- A truncation error estimate for global QBX expansions derived by Epstein et al., but involves an unknown constant.

Adaptive QBX

For a set of points $z \in \Omega$, we want to approximate

$$\varphi(z) = \frac{1}{2\pi} \int_{\Gamma} \mu(w) \mathrm{Im} \left\{ \frac{\mathrm{d}\, w}{w - z} \right\}$$

with an error no larger than a given tolerance *TOL*.

If z close enough such that a local QBX expansion will be formed:

Compute coefficient after coefficient on the fly.

For each coefficient, use error estimate to determine the upsampling.

Magnitude of coefficients will tell when to terminate.

af Klinteberg & T., ArXiv, 2017.

Adaptive QBX

- Working mode for AQBX:
  - For each term added to expansion, error decreases.

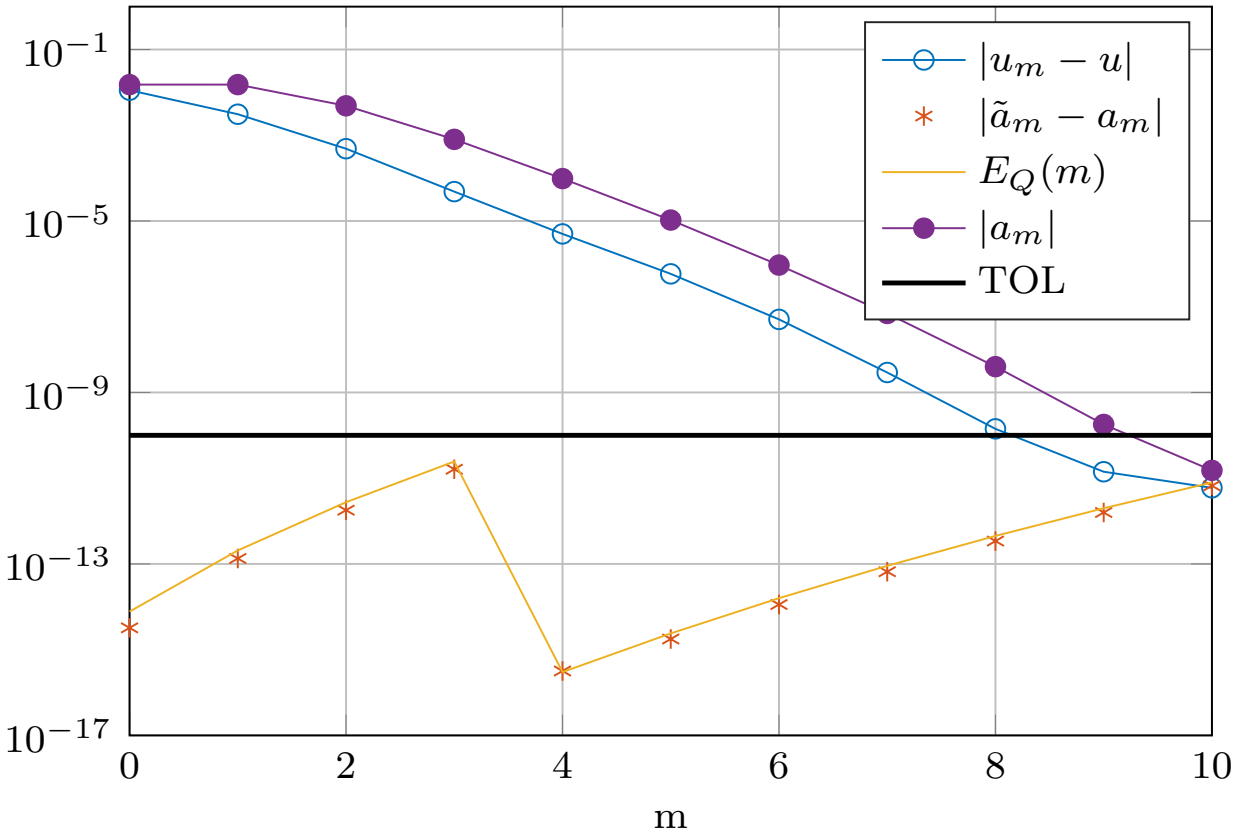

  - Coefficient error grows with m.
  - Shift to larger upsampling factor when error estimate predicts it is needed.

Results for Helmholtz equation

Solution $u(z)$ to the exterior Dirichlet problem

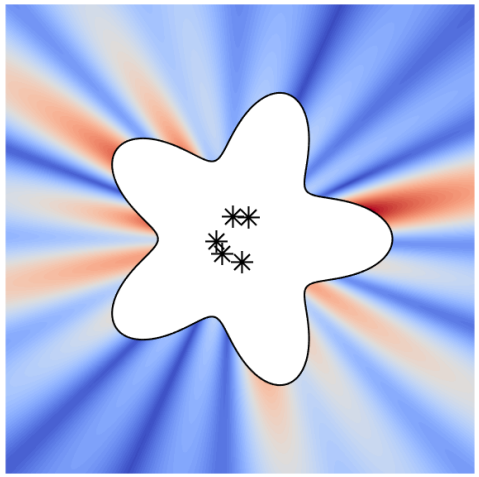

$|u(z)|$

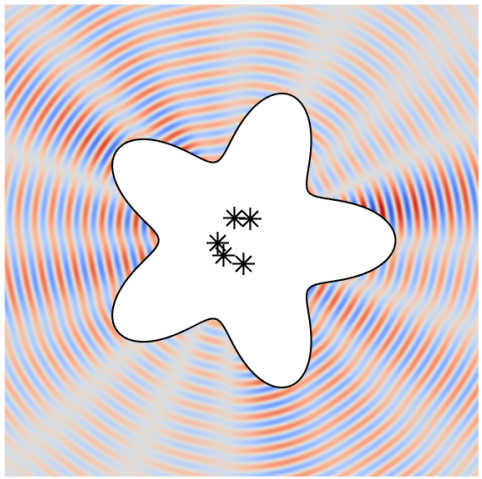

$\mathrm{Re}\, u(z)$

100 Gauss-Legendre panels of order *16* and equal arclength *h*.

Wave number $k = 4/h$.

Zoomed in error plots

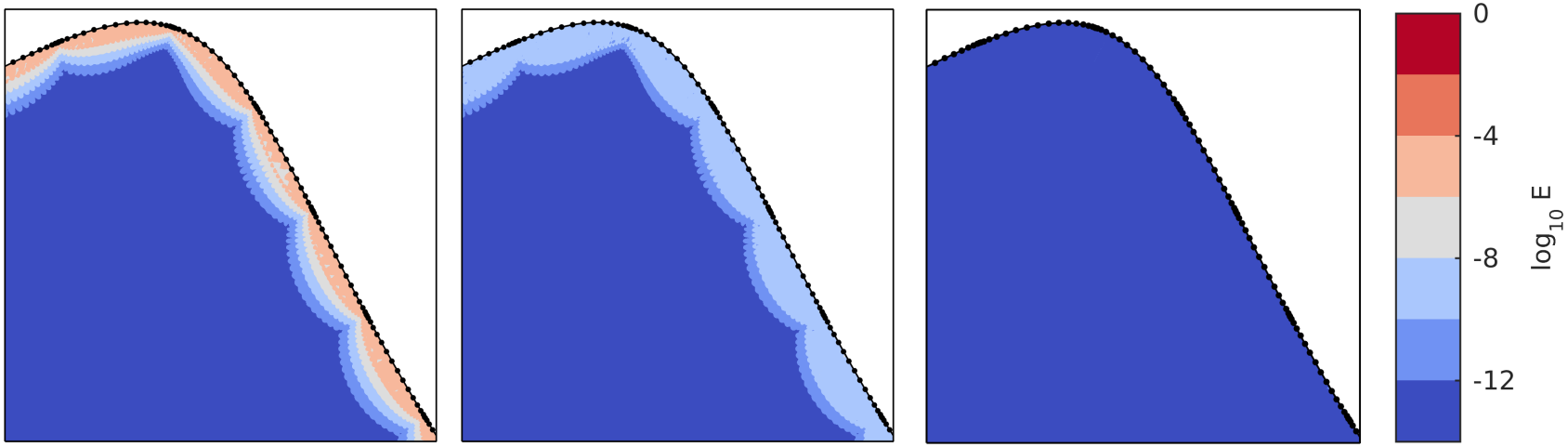

$TOL = 10^{-4}$ $TOL = 10^{-8}$ $TOL = 10^{-12}$

QBX in 3D

- Denote by Ω the domain exterior to a sphere, and consider

$$\mu \Delta \boldsymbol{u} = \nabla p, \qquad \nabla \cdot \boldsymbol{u} = 0 \qquad \boldsymbol{x} \in \Omega$$
$$\boldsymbol{u}(\boldsymbol{x}) = \bar{\boldsymbol{u}}(\boldsymbol{x}) \qquad \boldsymbol{x} \in \partial\Omega$$

- Double layer integral formulation solved to high accuracy, to obtain the source density **q,** defined on the surface of the sphere.

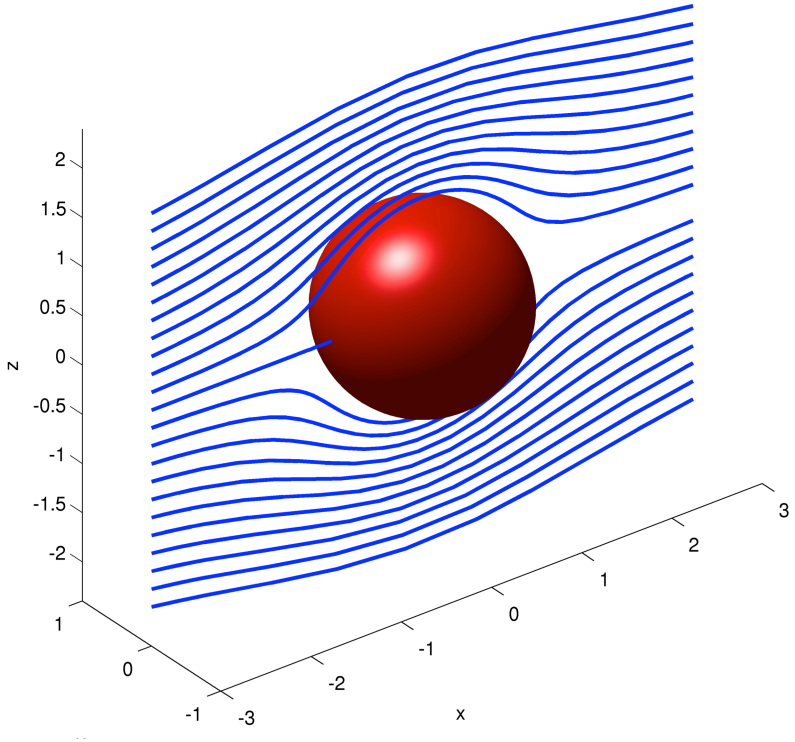

A slice of the exact solution for a sphere traveling to the left with constant speed.

Velocity $\boldsymbol{u}(\boldsymbol{x})$ for any $\boldsymbol{x} \in \Omega$ defined as

$$u_j(\boldsymbol{x}) = \int_{\partial\Omega} \boldsymbol{q}_l(\boldsymbol{y})\, T_{j\ell m}(\boldsymbol{x}-\boldsymbol{y})\hat{\boldsymbol{n}}_m(\boldsymbol{y})\, dS_{\boldsymbol{y}}, \qquad j = 1,2,3$$

$$T_{j\ell m}(\boldsymbol{r}) = -6\frac{r_j r_\ell r_m}{|r|^5}$$

The Stresslet double layer potential

The Stresslet potential

$$u_j(\boldsymbol{x}) = \int_{\partial\Omega} \boldsymbol{q}_l(\boldsymbol{y})\, T_{j\ell m}(\boldsymbol{x}-\boldsymbol{y})\hat{\boldsymbol{n}}_m(\boldsymbol{y})\, dS_{\boldsymbol{y}}, \qquad j = 1,2,3$$

can be expanded using its relation to the harmonic double layer potential

$$u_j(\boldsymbol{x}) = \sum_{\ell=1}^{3} \left(x_\ell \frac{\partial}{\partial x_j} - \delta_{j\ell} \right) D[q_\ell \boldsymbol{n} + n_\ell \boldsymbol{q}](\boldsymbol{x}) - \frac{\partial}{\partial x_j} D[y_m q_m \boldsymbol{n} + y_m n_m \boldsymbol{q}](\boldsymbol{x})$$

where $$D[\boldsymbol{\rho}](\boldsymbol{x}) = \int_\Gamma \boldsymbol{\rho} \cdot \nabla_y \frac{1}{|\boldsymbol{x}-\boldsymbol{y}|}\, dS_y$$

The three components of the Stresslet potential can be expanded using four expansions of the harmonic double layer potential.

Spherical harmonics expansion

The starting point is the spherical harmonics expansion of the harmonic potential, about a point **c,**

$$\frac{1}{|\boldsymbol{x}-\boldsymbol{y}|}=\sum_{\ell=0}^{\infty}\frac{4\pi}{2\ell+1}\sum_{m=-\ell}^{\ell}r_x^{\ell}\,Y_{\ell}^{-m}(\theta_x,\phi_x)\,\frac{1}{r_y^{\ell+1}}\,Y_{\ell}^{m}(\theta_y,\phi_y)$$

Source point ***y***,
Target (evaluation) point ***x***
Expansion center ***c***

The spherical coordinate system is centered at **c,**

$$(r_x,\theta_x,\phi_x)=\boldsymbol{x}-\boldsymbol{c},\qquad (r_y,\theta_y,\phi_y)=\boldsymbol{y}-\boldsymbol{c}$$

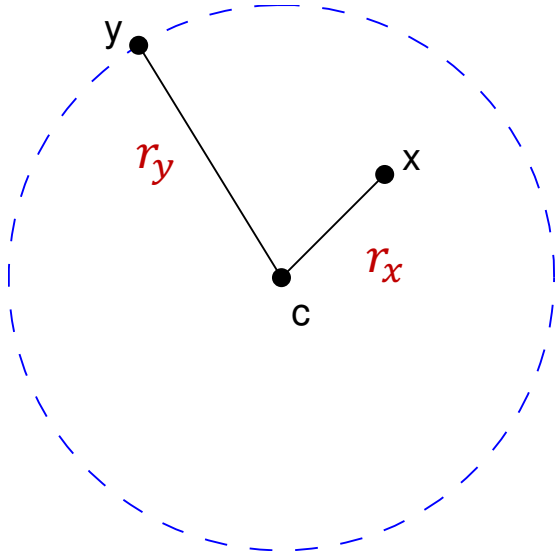

The expansion is valid for $|\boldsymbol{x}-\boldsymbol{c}|=r_x<r_y=|\boldsymbol{y}-\boldsymbol{c}|$.

$$Y_{\ell}^{m}(\theta,\phi)=\sqrt{\frac{2\ell+1}{4\,\pi}\frac{(\ell-|m|)!}{(\ell+|m|)!}}\underbrace{P_{\ell}^{m}(\cos\theta)}\;e^{im\phi}$$

Associated Legendre function

The Laplace double layer potential

For a Laplace double layer potential from a vector density $\boldsymbol{\rho}$

$$\Psi(\boldsymbol{c}) = D[\boldsymbol{\rho}](\boldsymbol{x}) = \int_{\Gamma} \boldsymbol{\rho} \cdot \nabla_y \frac{1}{|\boldsymbol{x}-\boldsymbol{y}|} dS_y$$

the expansion about $\boldsymbol{c}$ becomes

$$\Psi(\boldsymbol{x}) = \sum_{\ell=0}^{\infty} \frac{4\pi}{2\ell+1} \sum_{m=-\ell}^{\ell} r_x^{\ell} Y_{\ell}^{-m}(\theta_x, \phi_x) \underbrace{\int_{\Gamma} \boldsymbol{\rho} \cdot \nabla_y \frac{1}{r_y^{\ell+1}} Y_{\ell}^{m}(\theta_y, \phi_y)\, dS_y}_{\boldsymbol{\alpha}_l^m(\boldsymbol{c})}$$

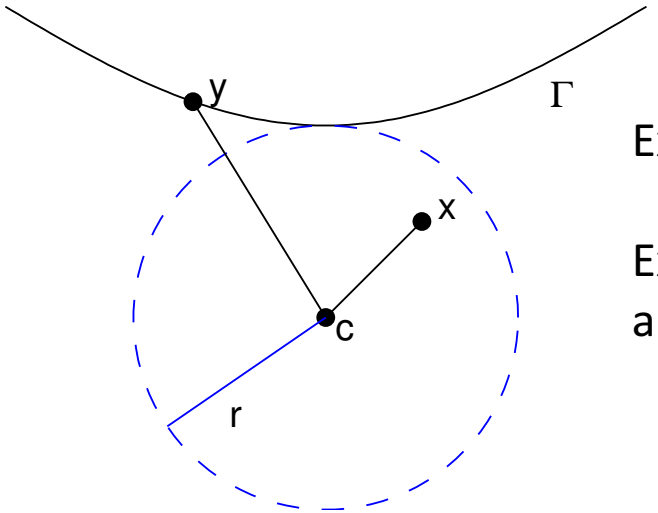

Expansion coefficients defined through smooth integrals.

Expansion valid inside sphere centered at **c** that touches Γ , and at intersection point of Γ and sphere.

Error in velocity field – introducing one expansion

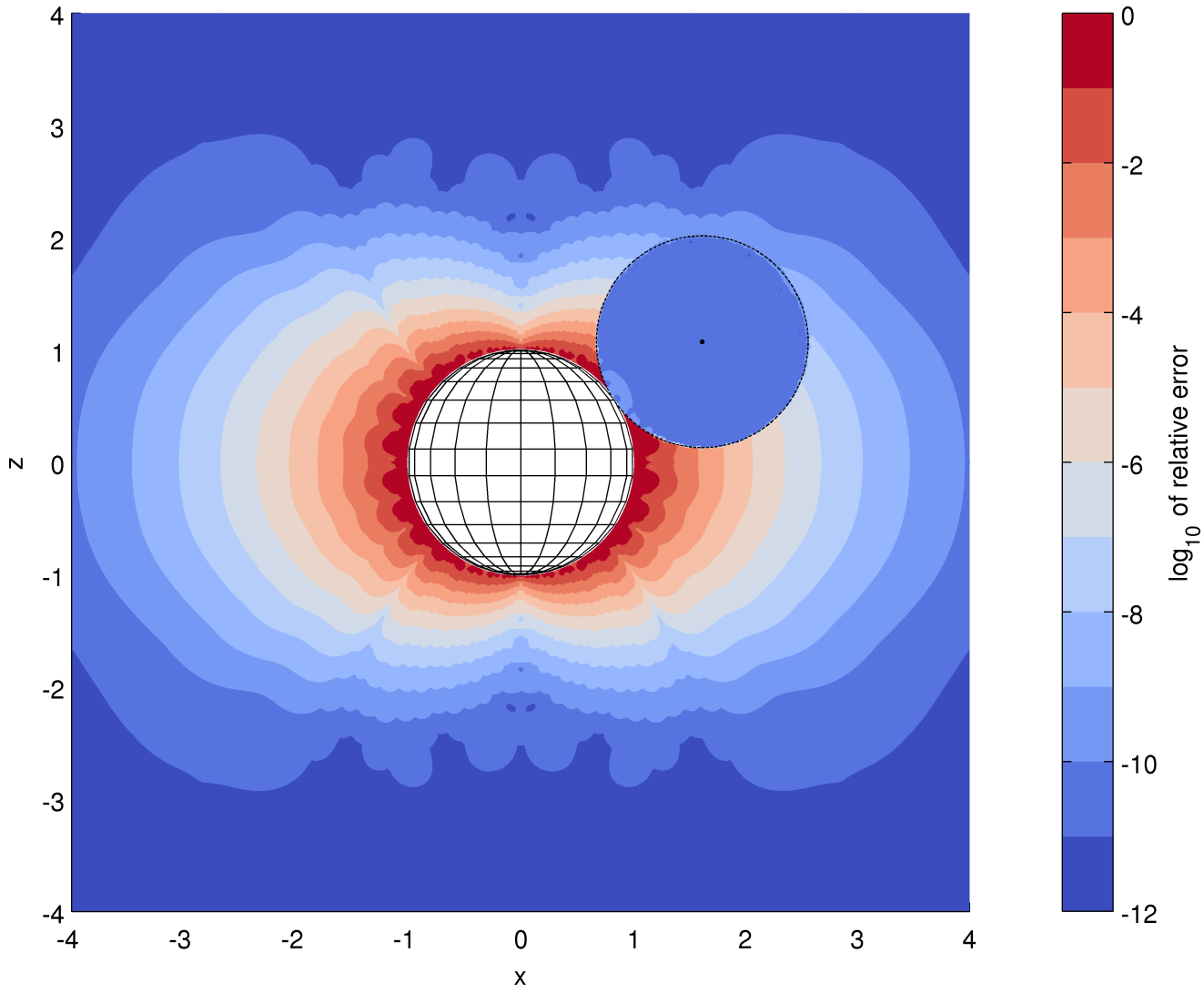

One spherical harmonics expansion is introduced. Within the expansion radius, the local expansion is evaluated instead of computing the integral directly.

QBX for the Stresslet

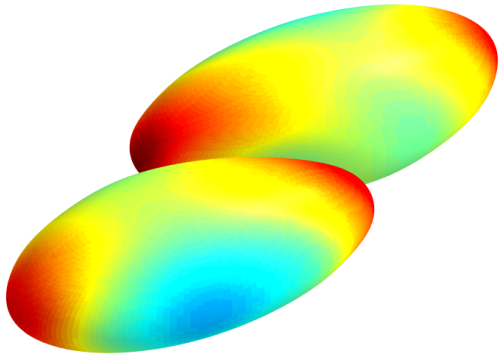

Expansion order p, upsampling factor κ.

- Truncate expansions at $\ell = p$, and evaluate coefficients by numerical quadrature.
- To reduce error: Interpolate double layer density to finer grid before computing integrals = upsample discretization of surface with upsampling factor κ.
- The accuracy is increasing with p and κ, but so is the computational cost.

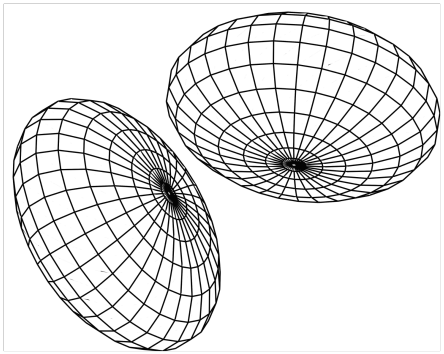

- First consider rigid bodies of a simple shape: spheroids.
  - Precompute to make evaluations faster.
  - Reduce storage by using geometric symmetries of the spheroids.
- Surface parameterization $\boldsymbol{x}(\theta, \varphi)$
  - Trapezoidal rule in φ, $0 \leq \varphi < 2\pi$
  - Gauss-Legendre quadrature in θ, $0 \leq \theta \leq \pi$.

Constructing an efficient quadrature method

- Spheroid discretized with $N = n_q \times n_f$ points, source density $\boldsymbol{q}$ defined in these points.
- Can construct a matrix A_i of size $3N_p \times 3N_p$ such that

$$\boldsymbol{z}_i = A_i \boldsymbol{q}$$

  yields the $3N_p$ expansion coefficients for center $\boldsymbol{c}_\mathrm{i}$.
- The upsampling has been "hidden" in A_i.

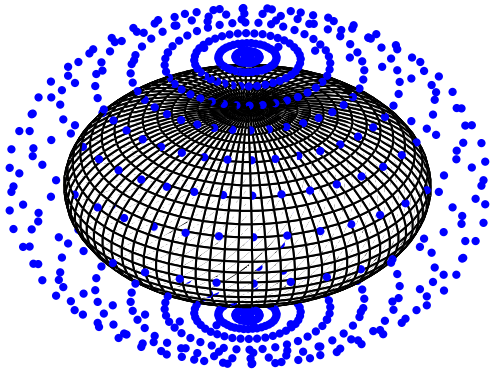

One center corresponding to each grid point

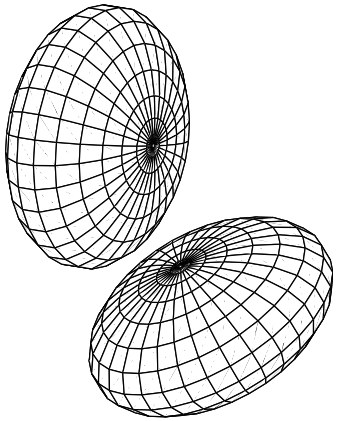

- Rotational symmetry: Only need to compute and save A_i for n_q expansion centers, mirror symmetry is reducing that to $n_q/2$.
- Each ellipsoid is the same modulo its orientation - precompute only for one reference body.

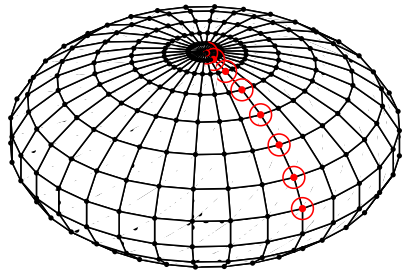

Rotation and mirror symmetry greatly reduces the need of precomputation.

QBX for solid spheroids in Stokes flow

- In 3D: no limit for the kernel on the surface. QBX used also to evaluate for “on-surface” target points, i.e. singular integrals.

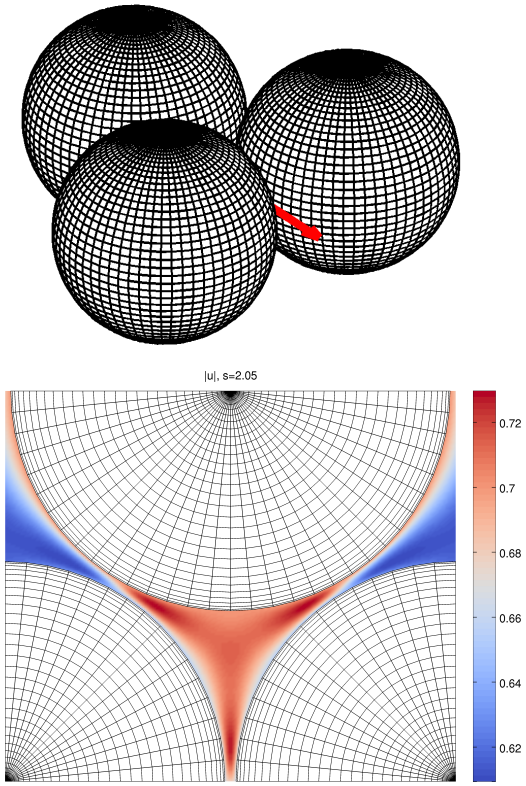

Validation case,

HJ Wilson, JCP 2013.

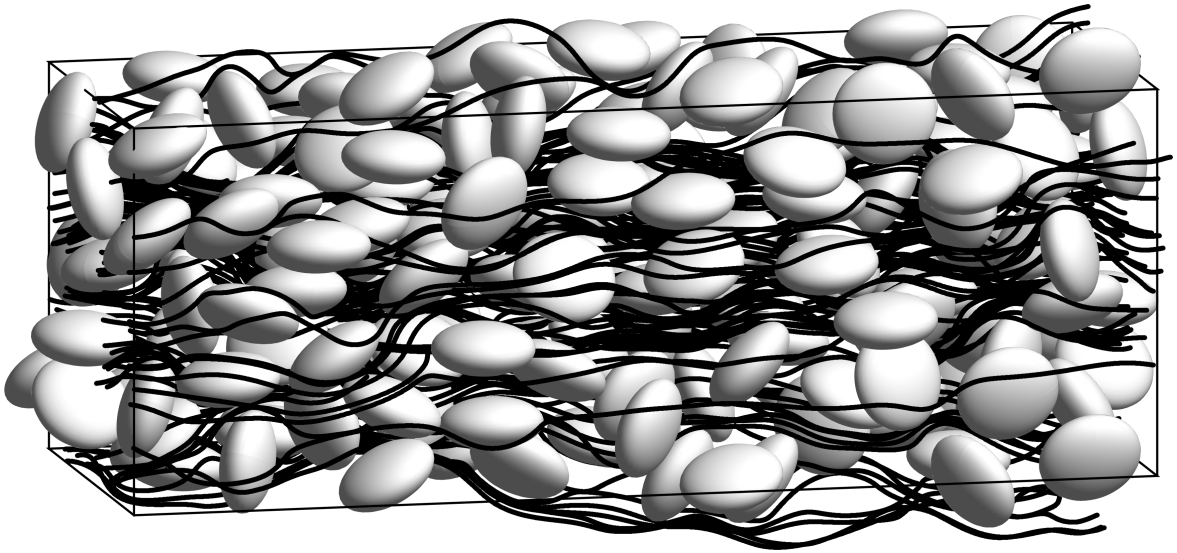

131 *randomly positioned oblate spheroids in a periodic box, at a volume concentration of* 24%*.*

Background flow entering from left.

Streamlines in black.

af Klinteberg & T., J. Comput. Phys., 2016.

What about drops in 3D?

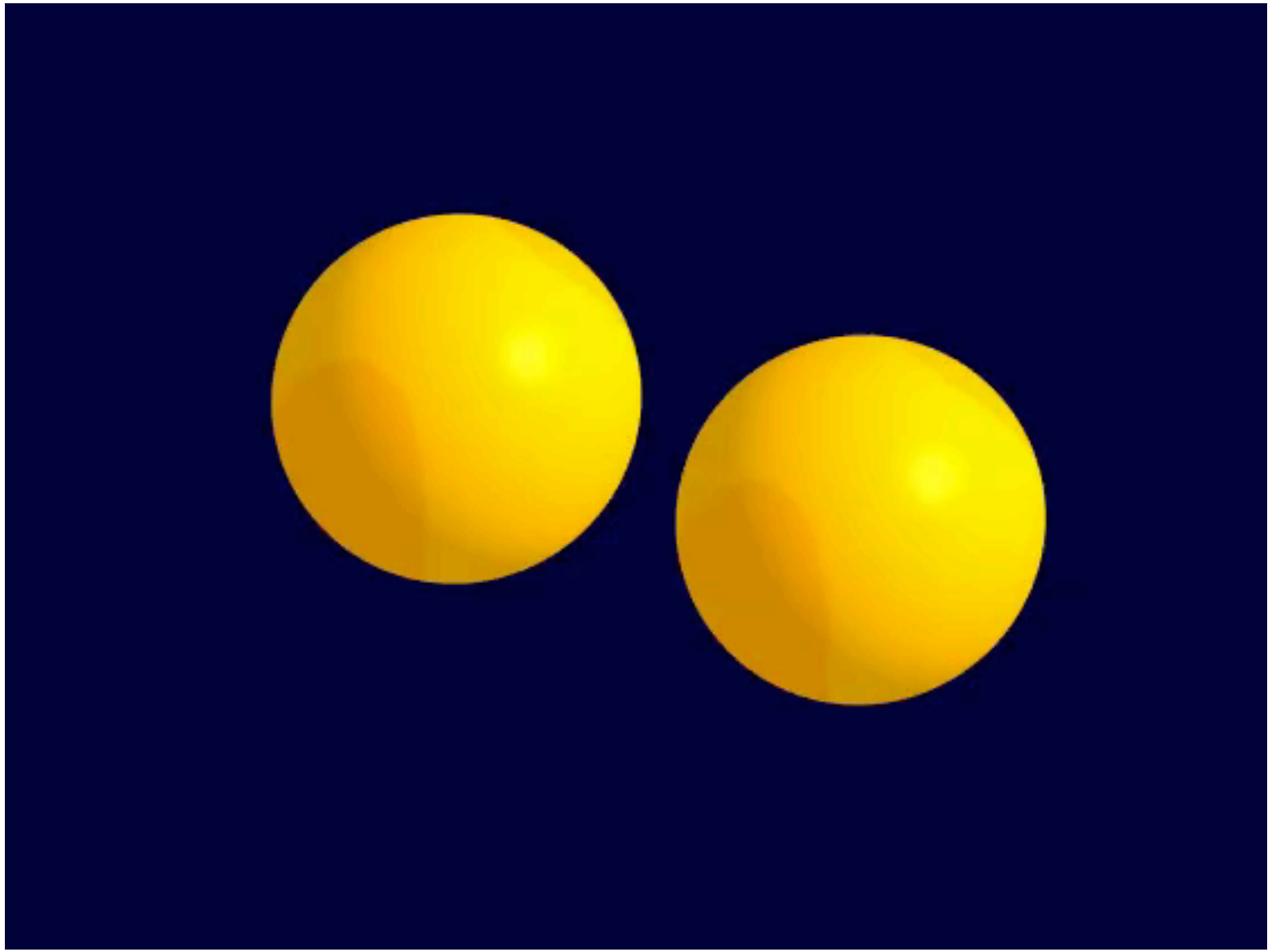

C. Sorgentone & T, ArXiv 2017.

Going further?

- QBX for solid spheroids:
  - Upsampling can be taken "sufficiently" large, cost hidden in precomputation (done for one spheroid only).
  - Expansion order affects computational cost and must be chosen.
- What about e.g. deformable drops?
  - Precomputation not possible, geometry of surface is time-dependent.
  - Cost of QBX will be large. For a given expansion order p, number of terms in sum is $\mathrm{O}(p^2)$.

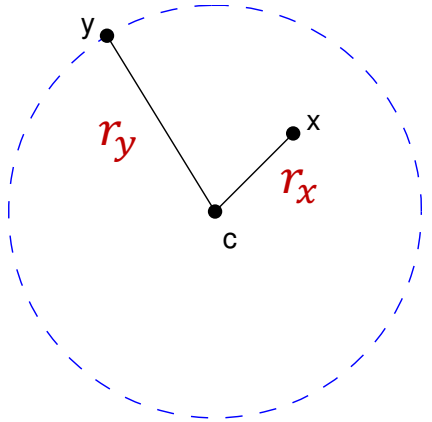

Expansion for Laplace double layer:

$$\boldsymbol{\alpha}_l^m(\boldsymbol{c}) = \int_\Gamma \boldsymbol{\rho} \cdot \nabla_y \frac{1}{r_y^{\ell+1}} Y_\ell^m(\theta_y, \phi_y)\, dS_y$$

$$\Psi(\boldsymbol{x}) \approx \sum_{\ell=0}^{p} \frac{4\pi}{2\ell+1} \sum_{m=-\ell}^{\ell} \boldsymbol{\alpha}_l^m(\boldsymbol{c})\, r_x^\ell\, Y_\ell^{-m}(\theta_x, \phi_x)$$

Separation between source and target:

- *Coefficients depend on sources.*

- *Expansion can be evaluated for different targets (within radius of convergence).*

Target specific expansions

- What if each expansion is used only once or a few times?
- Is it worth paying for separation between source and target?
- We have

$$\frac{1}{|\boldsymbol{x}-\boldsymbol{y}|}=\sum_{\ell=0}^{\infty}\frac{4\pi}{2\ell+1}\sum_{m=-\ell}^{\ell} r_x^{\ell}\, Y_{\ell}^{-m}(\theta_x,\phi_x)\,\frac{1}{r_y^{\ell+1}}\,Y_{\ell}^{m}(\theta_y,\phi_y)$$

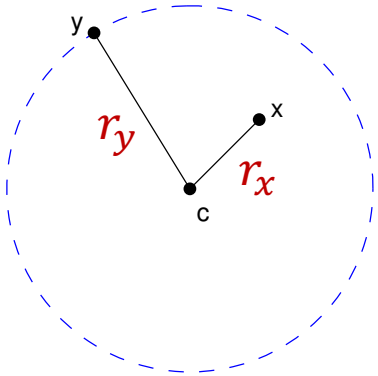

but what we really started with was

$$\frac{1}{|\boldsymbol{x}-\boldsymbol{y}|}=\sum_{\ell=0}^{\infty}\frac{r_x^{\ell}}{r_y^{\ell+1}}P_{\ell}\left(\cos\theta\right),$$

- P_ℓ: *Legendre polynomial of degree* ℓ.
- θ: *Angle between* $\boldsymbol{x}-\boldsymbol{c}$ *and* $\boldsymbol{y}-\boldsymbol{c}$.

- We can build a target specific QBX expansion from this expression (w M. Siegel)
  - Number of terms will be $p+1$ as compared to $O(p^2)$ for the same expansion.
  - Coefficients will be target specific, and can be used only for one target.

AQBX for deformable drops in 3D?

- Target specific expansions to reduce the number of terms in expansion.

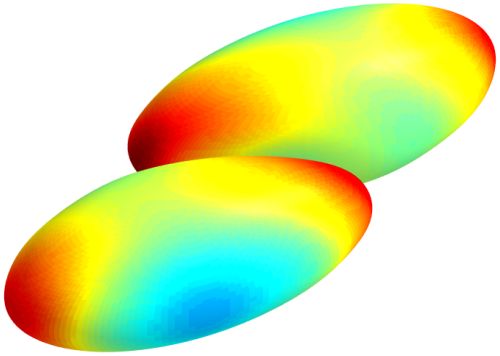

- Same idea as in 2D:
  - Expansion order determined on the fly, given an error tolerance.
  - For each coefficient, determine what upsampling is needed.

- For this: Need error estimates in 3D!

- Ongoing work with Ludvig af Klinteberg and Chiara Sorgentone.

Error estimates in 3D?

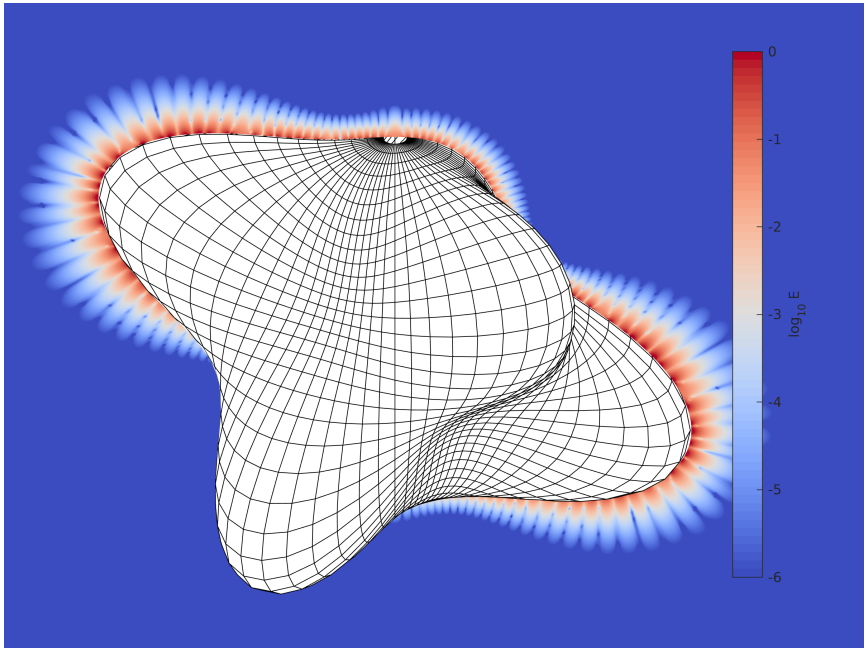

3D Laplace, exterior problem.
Measured errors, volume/slice.

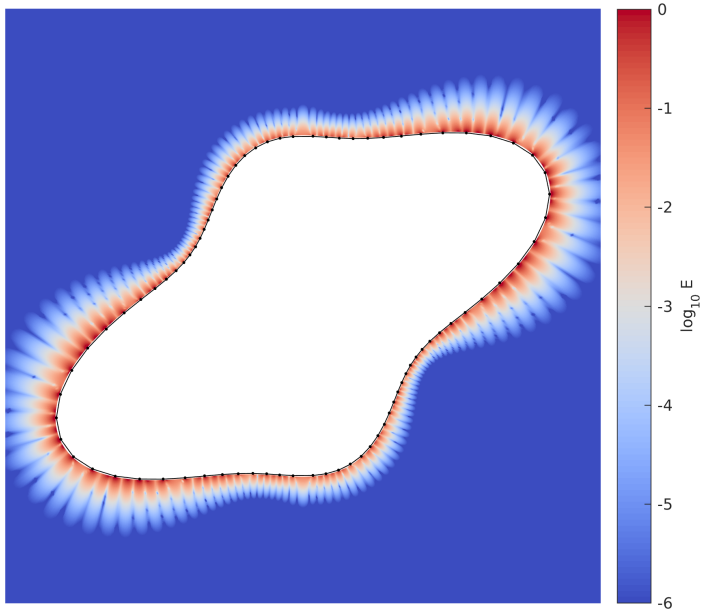

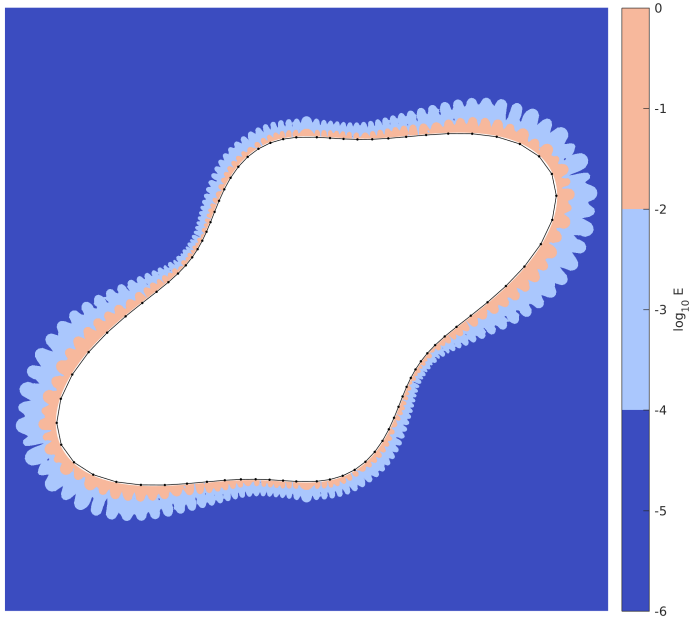

Discontinuous coloring to show error levels.

Error estimates in 3D?

First results are promising!

Colors:

Measured numerical errors.

Black contours:

Error estimate.

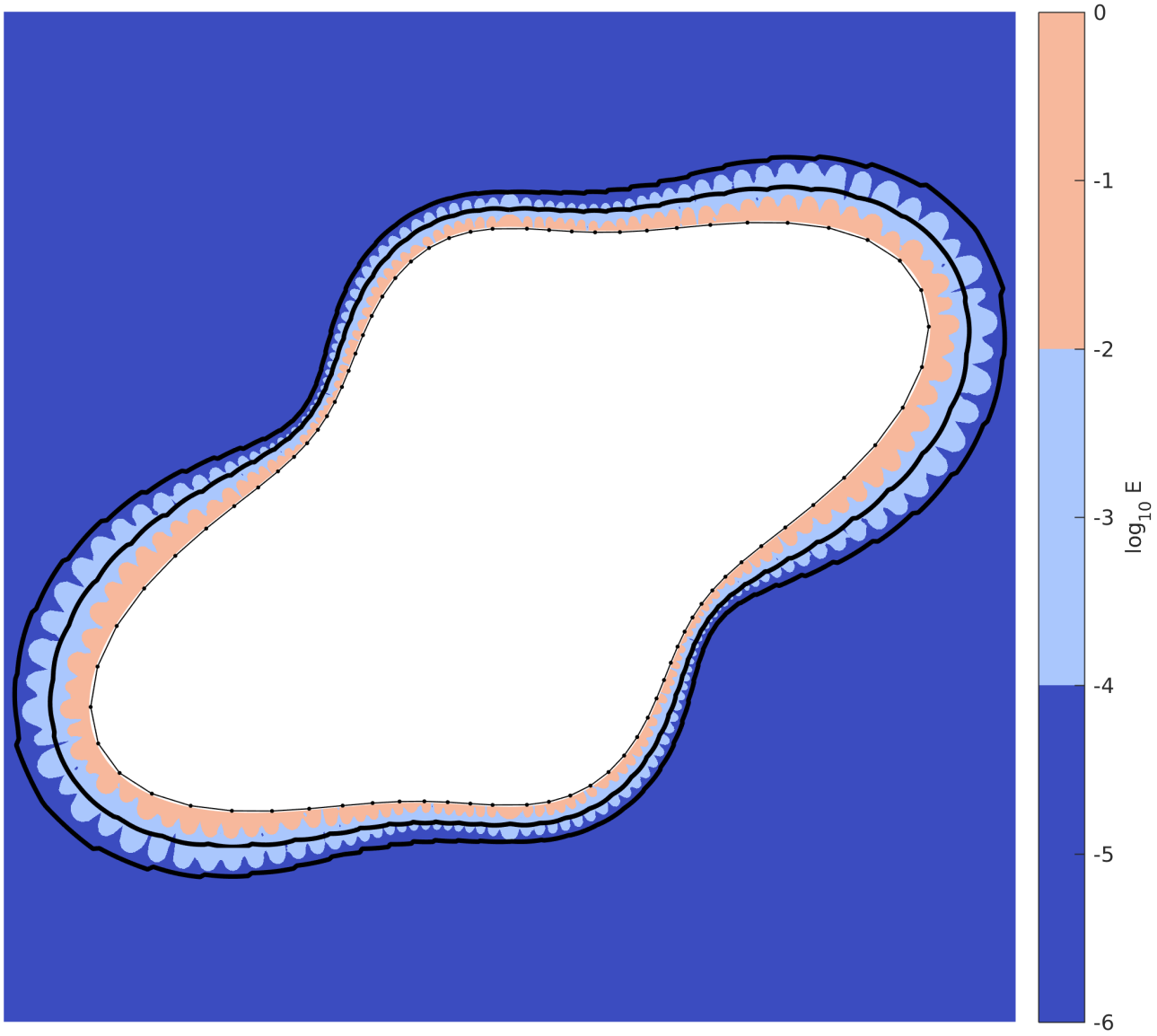

A few last comments…

- Development to integrate QBX into a fast multipole method (FMM).
  - Global QBX in 2D for Helmholtz equation: M. Rachh, A. Kloeckner and M. O'Neil. JCP, 2017.
  - Ongoing 3D work by A. Kloeckner.
- Order of expansions larger than in regular FMM to allow for shift of expansions to QBX centers.
- Many geometric considerations, a very complicated code.

- For general geometries, FMM-QBX should be the way to go!
- AQBX for drops, a "local" correction for each drop, might well come out faster for simulations with many drops with moderate resolution on each.
- Precomputed QBX (for geometries where possible) hard to beat.

Thank you!

Vetenskapsrådet

Knut och Alice Wallenbergs Stiftelse

Many thanks also to
Michael Siegel and Rikard Ojala!

Photo from Research Day in the archipelago of Stockholm July 4-5, 2017.

Upper row: Shriram Srinivasan, Chiara Sorgentone, Ludvig af Klinteberg, A-K T, Erik Lehto.
Lower row: Davoud Saffar Shamshirgar, Sara Pålsson, Fredrik Fryklund, Joar Bagge, Federico Izzo.

ROYAL INSTITUTE
OF TECHNOLOGY

Highly accurate numerical methods and error estimates for evaluation of nearly singular integrals in integral equations

Anna-Karin Tornberg
KTH Mathematics, Stockholm

SIAM Annual Meeting, July 10-14, 2017.

FLOW
LINNÉ FLOW CENTRE

SeRC

Evaluating velocity in domain

- Can be done as a post-processing step.
- At interface, jump in the double layer potential

$$\lim_{\varepsilon \to 0} K_D[\boldsymbol{u}](\boldsymbol{x} \pm \varepsilon \hat{\boldsymbol{n}}) = \mp 4\pi \boldsymbol{u}(\boldsymbol{x}) + K_D[\boldsymbol{u}](\boldsymbol{x}), \quad \boldsymbol{x} \in \Gamma$$

- Velocity formulas outside and inside drops differs,
  - Match at interface due to jump in double layer potential.

- Derivatives of velocities discontinuous at interfaces ($\lambda \neq 1$).
- Velocity divergence free by construction.

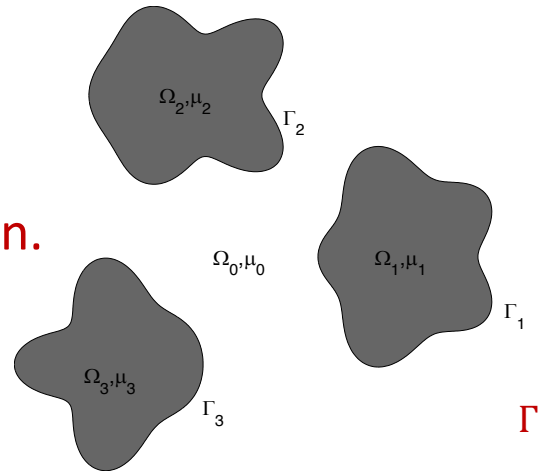

$$\Gamma = \bigcup_{m=1}^{M} \Gamma_m$$

- Including also solid boundaries yields coupled system with integrals both over fluid interfaces and solid boundaries.

Equations

$$\frac{1}{|\boldsymbol{x}-\boldsymbol{y}|} \approx \sum_{\ell=0}^{p} \frac{4\pi}{2\ell+1} \sum_{m=-\ell}^{\ell} r_x^{\ell}\, Y_{\ell}^{-m}(\theta_x,\phi_x)\, \frac{1}{r_y^{\ell+1}}\, Y_{\ell}^{m}(\theta_y,\phi_y)$$

$$\Psi(\boldsymbol{x}) \approx \sum_{\ell=0}^{p} \frac{4\pi}{2\ell+1} \sum_{m=-\ell}^{\ell} \boldsymbol{\alpha}_l^m(\boldsymbol{c})\, r_x^{\ell}\, Y_{\ell}^{-m}(\theta_x,\phi_x)$$

$$\boldsymbol{\alpha}_l^m(\boldsymbol{c}) = \int_{\Gamma} \boldsymbol{\rho} \cdot \nabla_y \frac{1}{r_y^{\ell+1}}\, Y_{\ell}^{m}(\theta_y,\phi_y)\, dS_y$$

$$\Psi(\boldsymbol{x}) \approx \sum_{\ell=0}^{p} \frac{4\pi}{2\ell+1} \sum_{m=-\ell}^{\ell} r_x^{\ell}\, Y_{\ell}^{-m}(\theta_x,\phi_x) \underbrace{\int_{\Gamma} \boldsymbol{\rho} \cdot \nabla_y \frac{1}{r_y^{\ell+1}}\, Y_{\ell}^{m}(\theta_y,\phi_y)\, dS_y}_{\boldsymbol{\alpha}_l^m(\boldsymbol{c})}$$

Stokes flow in 2D

- In the case of only drops, and no solid boundaries, we use a complex variable formulation (not as easy to dechifer as the one shown, see Kropinski, JCP, 2001).
- Solid boundaries add more terms in integral equation, must solve for unknown density on solid boundaries.

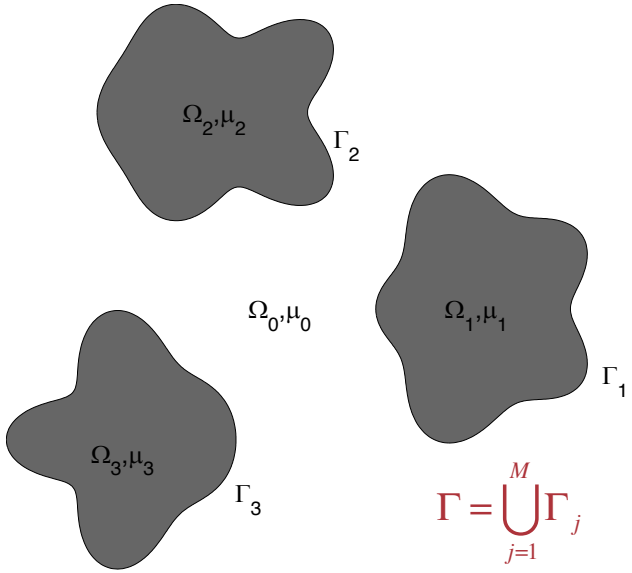

- In either case, write integrals in complex form and apply interpolatory quadrature when needed.
- Extension of Helsing & Ojala, see Ojala & T. , JCP 2015.

The integral

$$\int_\Gamma \boldsymbol{q}_\ell(\boldsymbol{x}) T_{j\ell m}(\boldsymbol{x}-\boldsymbol{y}) \boldsymbol{n}_m(\boldsymbol{y}) \mathrm{d}S_y$$

is equivalent to

$$\int_\Gamma \omega(\tau) \mathrm{Im}\left\{\frac{d\tau}{\tau - z}\right\} + \int_\Gamma \overline{\omega(\tau)} \frac{\mathrm{Im}\{(\bar{\tau}-\bar{z})\, d\tau\}}{(\bar{\tau}-\bar{z})^2}$$

where $\boldsymbol{q}_1 = \mathrm{Re}\{\omega\}$ and $\boldsymbol{q}_2 = \mathrm{Im}\{\omega\}$

The full method

- Hybrid method: switch between equidistant and Gauss-Legendre nodes using the non-uniform FFT (NUFFT).
- Adaptive 2nd order Runge-Kutta method for time-stepping.
- Global spatial adaptivity: keep Δs close to initial.
- No model for coalescence.

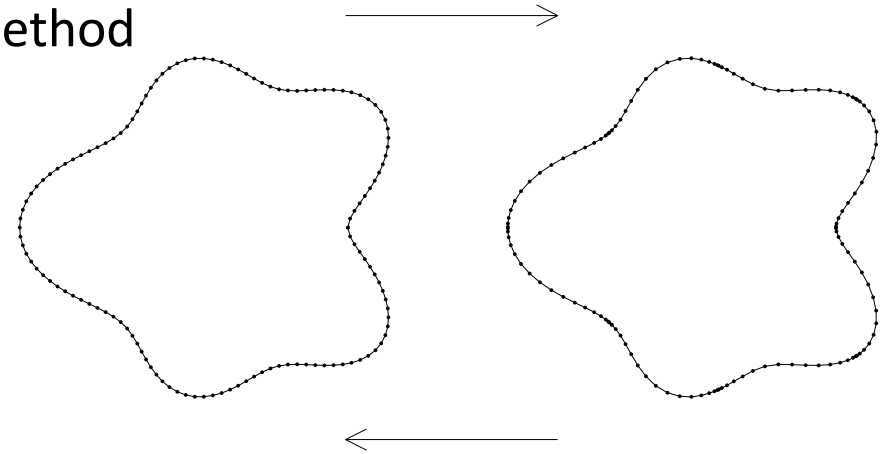

One time step

- Spectrally interpolate representation of curve from equidistant grid to Gauss Legendre panels (by NUFFT).
- Solve the integral equation based on Gauss-Legendre quadrature rule, GMRES and FMM/Spectral Ewald. Use special quadrature when needed.
- Interpolate velocities to equidistant grid.
- Solve for arclength preserving tangential velocity (FFTs on uniform grid).
- Update position of interfaces.

Two drops in shear flow

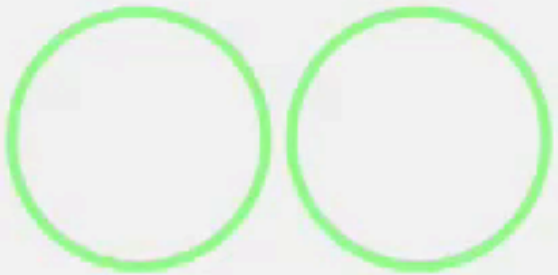

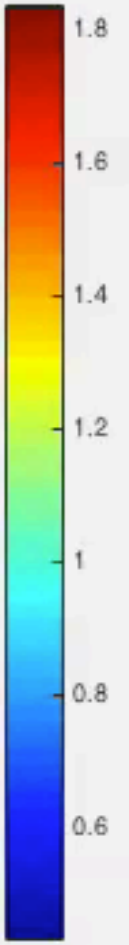

Clean drops as black contours.

Colored contours show concentration of surfactant that has been added to modified the surface tension (not discussed here, with Sara Pålsson).

Two drops in extensional flow

Clean drops as black contours.

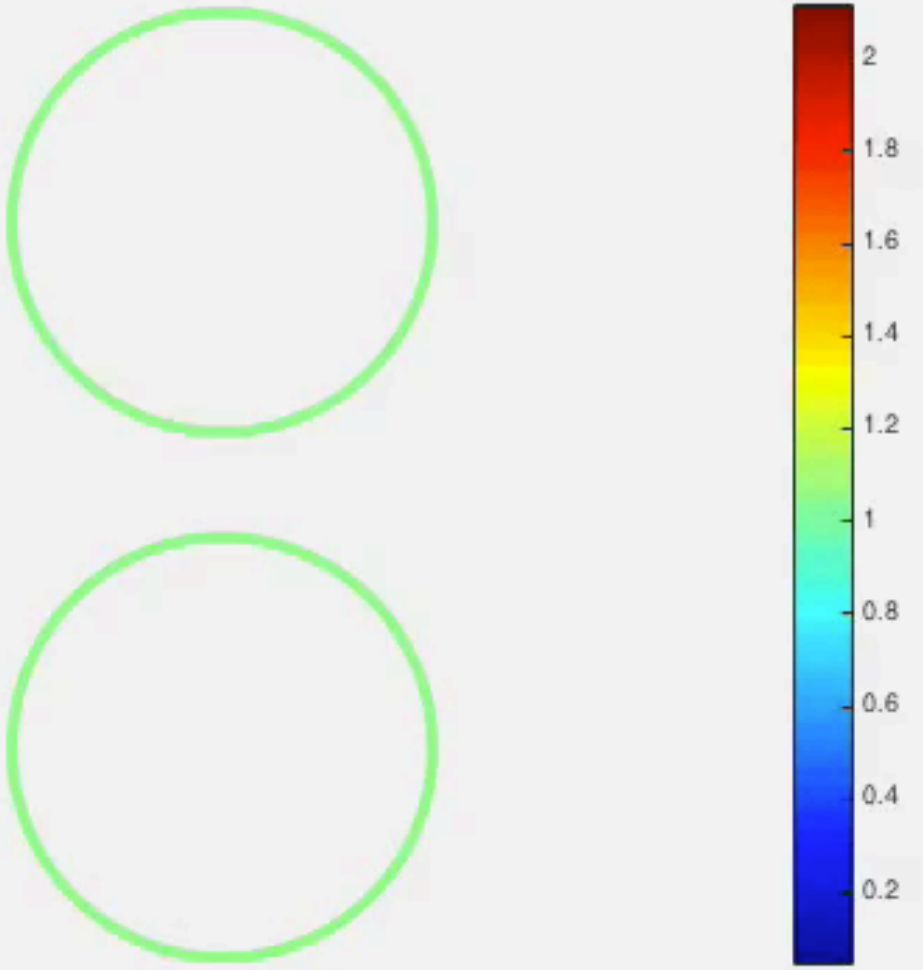

Colored contours show concentration of surfactant that has been added to modified the surface tension (not discussed here).

Error plots for Gauss-Legendre quadrature

$$g_p(x) = \frac{1}{((x-a)^2 + b^2)^p}$$

$n-$point Gauss-Legendre rule

$g_1(x) = ((x-0.1)^2 + (0.2)^2)^{-1}$

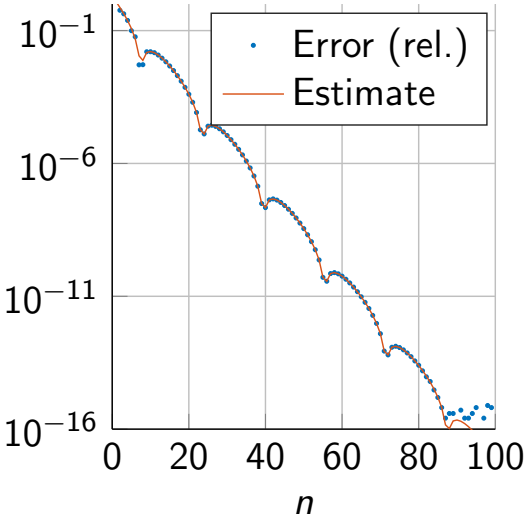

$g_1(x) = (x^2 + (0.2)^2)^{-1}$

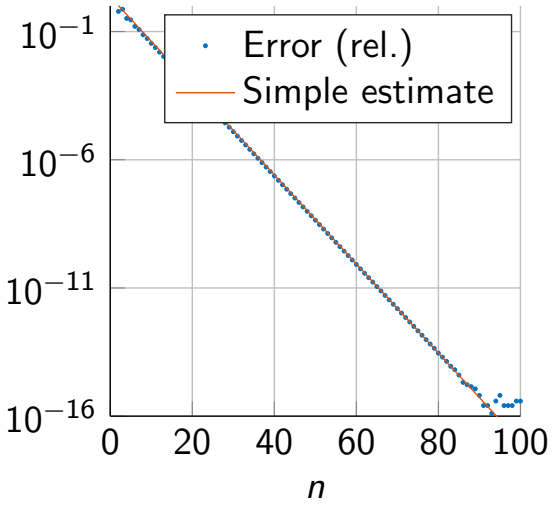

$g_5(x) = ((x-0.1)^2 + (0.2)^2)^{-5}$

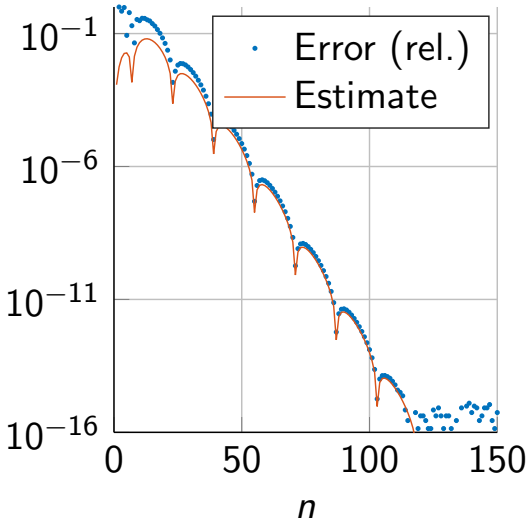

$$\left|R_n[g_p]\right| \simeq \frac{2}{(p-1)!(2b)^p} \left| \mathrm{Im}\left\{ \left(-\frac{2n+1}{\sqrt{z_0^2-1}} \right)^{p-1} \frac{2\pi}{\left(z_0 + \sqrt{z_0^2-1}\right)^{(2n+1)}} \right\} \right|$$

$$z_0 = a + ib$$

Simple estimate :

$$\left|R_n[g_p]\right| <\sim \frac{2\pi}{(p-1)!b^p} n^{p-1} e^{-2bn}$$

Estimates via contour integrals

- Can show that

  (Donaldson end Elliott, 1972),

$$R_n[f] = \frac{1}{2\pi i}\int_C f(z)k_n(z)\,\mathrm{d}z$$

  - $k_n(z)$ depends on the quadrature rule.
  - If f is a real function, $f(z)$ is a complex extension of f.
  - C is a contour that encloses Γ.

- Assuming $f(z)$ analytic on and within C.

- For a meromorphic function *f(z)* that is analytic everywhere except at points $\{z_1, \ldots, z_N\}$,

$$R_n[f] = \frac{1}{2\pi i}\int_C f(z)k_n(z)\,\mathrm{d}z - \sum_{j=1}^{N} \mathrm{Res}[f(z)k_n(z), z_j]$$

where C is now a large contour that we can take to infinity.

Estimates via contour integrals, contd

- For the n-point Gauss-Legendre rule

$$k_n(z) = \frac{1}{P_n(z)} \int_{-1}^{1} \frac{P_n(t)}{z-t}\, \mathrm{d}t$$

P_n: Legendre polynomial of degree n.

- No closed form, but in the limit $n \to \infty$

$$k_n(z) \cong \frac{2\pi}{\left(z + \sqrt{z^2-1}\right)^{2n+1}}$$

- Provides an accurate approximation also for moderately large n.
- Aiming for practical estimates, not bounds!
- Will consider functions

$$f_p(t) = \frac{1}{(t-t_0)^p}, \qquad t_0 = a + ib$$

$$g_p(t) = \frac{1}{\left((t-a)^2 + b^2\right)^p}, \qquad -1 < a < 1, 0 < b \ll 1$$